SOVIET PHYSICS

USPEKHI

A Translation of Uspekhi Fizicheskikh Nauk

SOVIET PHYSICS USPEKHI (Russian Vol. 92, Nos. 3 and 4) JANUARY-FEBRUARY 1968

621.378.325

SOLID STATE LASERS

A. A. MAK, Yu. A. ANAN'EV, and B. A. ERMAKOV

Usp. Fiz. Nauk 92, 373–426 (July, 1967)

I. INTRODUCTION

SOLID state lasers are a widely used class of generators of coherent optical radiation, presently delivering the maximum pulse power (up to 10^{10} W). We consider in this review the present status of the theory and technology of solid state lasers. The properties of the solid-state laser are determined by the characteristics of the active medium, the resonator, and the optical-pumping system.

Optically excited active media are of either the three-level or four-level type (Fig. 1). The optical pumping of the active medium produces level-population inversion. The gain at the center of the luminescence line is equal to

$$k = g\frac{\varkappa h\nu_g B_g}{c\Delta\nu_{lum}}\left(N_u - \frac{g_u}{g_l}N_l\right), \qquad (1)$$

where B_g is the Einstein coefficient for the stimulated emission at the working transition; ν_g is the emission frequency at the working transition; N_u, N_l, g_u, and g_l are the populations and the statistical weights of the upper and lower working levels, respectively; $\Delta\nu_{lum}$ is the width of the luminescence line at the working transition; g is a coefficient equal to $2/\pi$ for a Lorentz line contour and $(2/\pi)\sqrt{\pi \ln 2}$ for a Gaussian contour; $\varkappa$ is the refractive index of the medium.

Generation is produced if the losses in the resonator are compensated by the gain in the active medium (threshold condition) [1]:

$$\exp(2lk_{thr} - \sigma) R_1 \cdot R_2 = 1, \qquad (2')$$

or

$$\delta = \left(N_u - \frac{g_u}{g_l}N_l\right)_{thr} = \frac{c\Delta\nu_{lum}(\sigma + \ln 1/R_1R_2)}{g\varkappa h\nu_g B_g \cdot 2l}, \qquad (2)$$

where δ is the threshold population inversion; R_1 and R_2 are the reflection coefficients of the resonator mirrors; l is the length of the rod; σ are the losses per double pass, connected with the resonator Q by the relation

$$Q = \frac{\nu_g}{\Delta\nu_r} = \frac{4\pi\varkappa l\nu_g}{c\left(\sigma + \ln\frac{1}{R_1 \cdot R_2}\right)}.$$

As a rule, in a laser the width of the resonator band $\Delta\nu_r \ll \Delta\nu_{lum}$, and the dimensions of the resonator are much larger than the generation wavelength, so that a large number of oscillation modes can be excited. The main characteristics of these modes (spectral, spatial, damping, etc.) are determined primarily by the properties of the resonator [1-4]. The number of excited modes with different axial indices determines the spectral width of the laser emission, and that with different angular indices determines the angular divergence of the laser emission.

This number is determined, in turn, primarily by the spatial competition of the modes, which results from the saturation of the inverted population.[5,6].

The temporal characteristics and, accordingly, the temporal coherence of the laser emission are determined apparently by the effects of mode interaction in the resonator filled with the active medium [7,8,19].

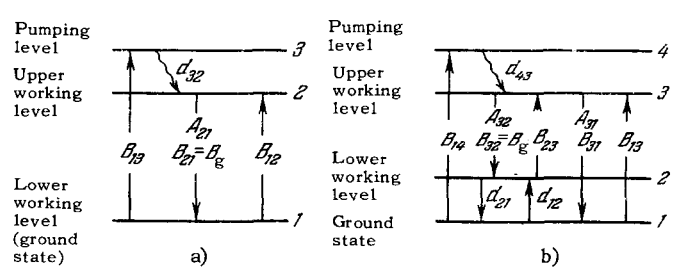

FIG. 1.

A characteristic feature of solid-state lasers is the "spike" emission character.

The operating conditions of solid-state lasers can be stationary and nonstationary. The former include continuous generation and amplification (the pumping is by sources of constant light), and also pulsed operation in which the pumping is by sources of light with pulse durations much larger than the lasing transient time. Stationary operation is characterized by constant laser parameters averaged over the spikes.

The nonstationary operation includes monopulse (MP) operation, which is produced by introducing into the resonator a shutter that changes rapidly the Q of the resonator (this makes it possible to obtain a powerful short-duration generation pulse), the pulse-amplification operation, and pulsed generation with short-duration or rapidly varying pumping.

II. THEORETICAL PRINCIPLES OF LASER DESIGN

To calculate the laser parameters, extensive use is being made presently of the method of kinetic equations (the probability method). The characteristics of the quantum-mechanical system (the active medium) are described by introducing appropriate transition probabilities. In the elementary theory, the properties of the resonator are taken into account by introducing effective loss σ (the single-mode approximation)[9-13]. It is assumed here that the generation emission density is distributed uniformly over the volume of the resonator, and the time of spectral relaxation of the luminescence line is short compared with the times characteristic of the development of the generation process, i.e., the line is homogeneously broadened. In spite of the simplicity of this model, it makes it possible to analyze the energetics of the processes in the laser and the connection between the energy parameters of the laser and the characteristics of the active medium, the resonator, and the pump.

When allowance is made for the spatial distribution of the radiation density of the individual modes and the loss corresponding to them, the kinetic-equation method makes it possible to estimate, besides the energy characteristics, also the spectral region and the angular divergence of the laser emission (the multi-mode approximation)[5,6,14-16]. In the case of spike emission, the kinetic equation calculations yield laser characteristics that are averaged over these spikes.

The most complete description of the laser characteristics is obtained by using the density-matrix method (e.g.,[7,8,17-19]). In this case, account is taken of the phase relations of the excited modes, so that the question of the mode interaction can be considered more correctly. It is possible that the "spike" structure of the solid-state laser emission can be interpreted only within the framework of such an analysis [7,8,19]. However, because of its complexity, this method has been developed so far only for highly simplified cases and cannot be used to calculate the main laser characteristics. We present in this section the main results obtained by the kinetic-equation method. The derivation of the kinetic equations from the equations for the density matrix, and the criteria for the applicability of the probability method, are considered in [18,20]. In the following sections we shall compare the experimental results with the deductions of the developed theory. For simplicity, we shall assume henceforth $g_1 = g_2$, $R_1 = 1$, and $R_2 \equiv R$ (see (1) and (2)).

1. Single-mode Approximation

We write down the population balance equation for a four-level active medium (see Fig. 1):

$$N_1+N_2+N_3+N_4=N_0;$$

$$\frac{dN_4}{dt}=u_{14}B_{14}(N_1-N_4)-\frac{1}{\eta_1}d_{43}N_4;$$

$$\frac{dN_3}{dt}=d_{43}N_4+u_{32}B_{23}(N_2-N_3)-\frac{A_{32}}{\eta_2}N_3;$$

$$\frac{dN_2}{dt}=d_{12}N_1-d_{21}N_2+u_{32}B_{32}(N_3-N_2)+N_3A_{32}+N_4A_{42},$$

where N_0 is the concentration of the activator particles; N_1, N_2, N_3, and N_4 are the level populations; A and B with indices are the Einstein coefficients for the corresponding transitions; d with indices are the probabilities of nonradiative transitions; u_{14} and u_{32} are the pump and generation densities; $\eta_1 = d_{43}/p_4$ is the quantum yield of excitation of the upper working level 3; $\eta_2 = A_{32}/P_3 = A_{32}\tau$; p_4 and p_3 are the total probabilities of the transitions from levels 4 and 3; τ is the lifetime of the excited state; $\eta = \eta_1\eta_2$ is the luminescence quantum yield of the line with frequency $\nu_{32} = \nu_g$.

If the following inequalities are satisfied:

$$d_{43} \gg u_{14}B_{14};\ d_{43} \gg \frac{1}{\tau};\ d_{21} \gg u_{14}B_{14}+A_{42}+\frac{1}{\tau};$$

$$\frac{N_2}{N_3}=\frac{d_{12}}{d_{21}}\frac{N_1}{N_3}=\frac{N_1}{N_3}e^{-\frac{h\nu_{21}}{kT}} \ll 1,$$

then the foregoing system of equations can be written in the form

$$\left.\begin{aligned} N_1+N_3&=N_0,\\ \frac{dN_3}{dt}&=\eta_1 u_p B_p N_1-u_g B_g N_3-\frac{N_3}{\tau}. \end{aligned}\right\} \qquad (3)$$

The indices "p" and "g" corresponding to the pumping and generation channels have been introduced in lieu of the indices "14" and "23."

We can obtain similarly a simplified system of equations for a three-level active medium:

$$\left.\begin{aligned} N_1+N_2&=N_0,\\ \frac{dN_2}{dt}&=\eta_1 u_p B_p N_1-u_g B_g (N_2-N_1)-\frac{N_2}{\tau}. \end{aligned}\right\} \qquad (4)$$

The use of the simplified systems of equations (3) and (4) makes it possible to obtain simple finite expressions for the laser parameters. At the same time, it should be taken into account that the assumptions made in their derivation are satisfied, as a rule, be-

cause of the large probabilities of the corresponding non-radiative transitions. Allowance for the encountered deviations entails no difficulty and will be presented below.

Using the population balance equations and the threshold relation (2), we can find expressions for the threshold pump-radiation density u_{thr} and the generation-radiation density u_g, and using the relations

$$P_{thr} = h\nu_p B_p N_1 l \int_S u_{thr}\, dS, \quad (5)$$

$$P_g = \frac{c}{2\varkappa} \ln \frac{1}{R} \cdot \Delta\nu_{lum} \frac{\eta_1 B_p}{B_r} \frac{N_0 - \delta}{\delta} \int_S (u_p - u_{thr})\, dS, \quad (6)$$

we can find the threshold pump radiation power P_{thr} absorbed in the medium and the generation power P_g [11] (ν_p is the pump radiation frequency; S is the cross section area of the rod). Expression (6) holds for $R \gtrsim 0.3$; at lower values of R, the uneven distribution of the radiation density u_g along the resonator becomes appreciable (greater than 20%) and the expression for P_g becomes more complicated (see [21,22]).

Let us consider the singularities of the solution for the basic laser regimes.

Stationary regime [9,11,22-25]. The expressions for P_{thr} and P_g are listed in Table I. For such four-level media as neodymium glass, $CaWO_4 : Nd^{3+}$, etc., we usually have $N_2/N_3 \ll 1$; for three-level media, as a rule, $\delta \ll N_0$. Therefore the threshold pump power in three-level media depends quite weakly on the Q of the generator, and in four-level media this dependence is strong. It follows from (7) and (8) that the ratio of the threshold pump powers for three- and four-level media is proportional to $(1/2)(1 + N_0/\delta)$, and inasmuch as $N_0/\delta \gtrsim 10$ the threshold for four-level media is much lower than for three-level media [24]. From (7), (8), and (9) we can readily obtain the optimal value of the reflection coefficient R_0 at which the generation power reaches a maximum value P_0 [11]. The expressions for R_0 and P_0 for a four-level medium are listed in Table Ia.

Under the assumptions made concerning the probabilities of the nonradiative transitions, the generation power depends strongly on the pump power. On the other hand, if the probabilities are not very large, then the linear dependence is violated. Thus, P_g reaches saturation, with increasing pump, when the following condition is satisfied [26]

$$n \gg \frac{N_0 \tau}{2\delta} \frac{d_{43} d_{21}}{d_{21} + d_{43}}. \quad (12)$$

As will be shown in Sec. IV.1, with neodymium glass as an example, these conditions are not satisfied for the available pump sources, so that the proportionality of P_g to $P_p - P_{thr}$ is not violated.

Pulsed regime. In this regime we distinguish between two stages—below the threshold and generation. In the former, excitation is accumulated until the population inversion δ is produced; in this stage we have in first approximation $u_g = 0$ (see the discussion of superluminescence below). Generation is delayed by t_{thr} relative to the instant of the start of pumping. For the case of a square pump pulse of duration t_{pul} and $t_{thr} \ll \tau$, the expressions for the threshold pump energy W_{thr} absorbed in the rod and the generation energy W_g are listed in Table Ib.

Before we proceed to the MP regime and the amplification regime, let us first discuss superluminescence.

Superluminescence. In the case of considerable population inversion, the medium has a large gain,

Table Ia

Regime	Four-level medium	Three-level medium
Stationary	$P_{thr} = h\nu_p l S \left[\frac{N_0}{\eta_1 \tau} e^{-\frac{\Delta E}{kT}} + 4\pi \frac{\varkappa^2 \nu_g^2 \Delta\nu_{lum} (\sigma + \ln 1/R)}{c^2 l \eta g} \right] \simeq \left(\frac{N_2}{N_3} \ll 1 \right) \simeq \frac{4\pi\varkappa^2 h}{c^2 g} \frac{S\nu_p \nu_g^2 \Delta\nu_{lum}}{\eta} (\sigma + \ln 1/R)$. (7)	$P_{thr} = \frac{1}{2} h\nu_p l S \left[\frac{N_0}{\eta_1 \tau} + 4\pi \frac{\varkappa^2 \nu_g^2 \Delta\nu_{lum} (\sigma + \ln 1/R)}{c^2 l \eta g} \right]$. (8)
	$P_g = \eta_1 \frac{\nu_g}{\nu_p} \frac{\ln 1/R}{\sigma + \ln 1/R} P_p \left(1 - \frac{1}{n}\right)$. (9)	
	$\ln 1/R_0 = \sigma(\sqrt{n_0} - 1)$. (10)	
	$P_{g_0} = \eta_1 \frac{\nu_g}{\nu_p} P_p \left(1 - \frac{1}{\sqrt{n_0}}\right)^2$. (11)	

Remark. $n = P_p/P_{thr}$ is the pump-power excess over threshold. n_0 is the excess over threshold for R = 1. $n_W = W_p/W_{thr}$ is the excess over the pump-energy threshold. ΔE is the energy gap between the lower working level and the ground level.

Table Ib

Regime	Four-level medium	Three-level medium
Pulsed	$t_{thr}=\tau\ln\frac{n}{n-1}\simeq(t_{thr}\ll\tau)\simeq\frac{\tau}{n}$. (13)	$t_{thr}\mid_{t_{thr}\ll\tau}\simeq\frac{\tau}{n}\frac{1-\delta/N_0}{1+\delta/N_0}\times\ln\frac{2}{1-\delta/N_0}$. (14)
	$W_{thr}=P_p\frac{t_{thr}}{1-e^{-\frac{t_{thr}}{\tau}}}\simeq(t_{thr}\ll\tau)\simeq P_{thr}\tau=\frac{4\pi\varkappa^2h}{c^2g}\times\frac{S\nu_p v_g^2\Delta\nu_{lum}\tau(\sigma+\ln 1/R)}{\eta}$. (15)	$W_{thr}\mid_{t_{thr}\ll\tau}\simeq P_{thr}\tau=\frac{1}{2}h\nu_p\times lS\left[\frac{N_0}{\eta_1}+4\pi\frac{\varkappa^2v_g^2\Delta\nu_{lum}\tau(\sigma+\ln 1/R)}{c^2l\eta g}\right]$ (16)
	$W_g\mid_{t_{thr}\ll\tau}\simeq\eta_1\frac{v_g}{v_p}\frac{\ln 1/R}{\sigma+\ln 1/R}W_p\left(1-\frac{1}{n_W}\right)$. (17)	

and then the spontaneous-emission quanta can give rise, before leaving the medium, to a large number of induced transitions, thereby reducing the stored excitation energy [27-33]. This effect, which is called superluminescence, is particularly important in MP and amplification regimes, and also in the stationary or pulsed regimes when the resonator mirrors have a small reflection coefficient. A reduction in the excited-state lifetime, due to superluminescence, was observed in [27-30], and a calculation of superluminescence is given in [28, 31-33].

For a four-level medium with a fixed lower level we get from (3)

$$\eta_1(N_0-N)B_p u_{thr}=\frac{N}{\tau}\gamma,$$

where N is the inverted population, which in this case is equal to N_3; $\gamma=\tau/\tau_e=1+\eta_2N_{st}/N_{sp}$; N_{st} and N_{sp} are the numbers of the acts of stimulated and spontaneous emission (due to spontaneous quanta) corresponding to the working transition. The quantity $\xi\equiv N_{st}/N_{sp}$, together with γ, depends on the degree of inversion and on the geometry of the active rod. From the last expression we can readily obtain an expression for the inverted population:

$$N^0=\frac{n\delta}{\gamma+(n-\gamma)\delta/N_0},\qquad(18)$$

where δ is the threshold inversion in the presence of the resonator. In analogy, we can obtain for a three-level medium

$$N^0=\frac{n-\gamma+(n+\gamma)\delta/N_0}{n+\gamma+(n-\gamma)\delta/N_0}N_0.\qquad(19)$$

Obviously,

$$\xi=\frac{\int_\nu\xi(\nu)k_\nu d\nu}{\int_\nu k_\nu d\nu},$$

where k_ν is the gain at the frequency ν; $\xi(\nu)$ is the number of stimulated transitions due to the spontaneous quantum of this frequency. To estimate $\xi(\nu)$ we can use the concept of the effective length l_{eff}, equal to the average path traversed by the spontaneous quantum before leaving the rod [28, 29, 33]:

$$\xi(\nu)=\frac{k_\nu}{k_\nu-\rho}[\exp(k_\nu-\rho)l_{eff}-1],\qquad(20)$$

where ρ is the loss coefficient in the rod per unit length. The approximate values of l_{eff} for rods of cylindrical form are listed in Table II.

For a cylindrical sample with a polished ($\alpha=0$) or roughened ($\alpha\simeq0.5$) side surface, a more correct calculation leads to the expression [33]

$$\xi(\nu)=\frac{k_\nu}{k_\nu-\rho}\left\{\frac{(1-\alpha)\exp\left[\frac{2}{3}D(k_\nu-\rho)\right]}{1-\alpha\exp[D(k_\nu-\rho)]}-1\right\}.\qquad(21)$$

More accurate calculation methods are considered in [28, 32, 33]. The calculated values of $\xi(\nu)$ and ξ for

Table II

Characteristic of rod	l_{eff}
Rod with polished side surface	$l_{eff}\simeq l$
Rod of diameter D surrounded by an immersion sheath of diameter D_0 with polished outer surface, $l/D\geq10$.	$l_{eff}\simeq\frac{2}{3}D+\frac{4}{3\pi}\frac{l\ln\varkappa}{\frac{D_0}{D}-\frac{D}{8D_0}}$
Rod with translucent ($\alpha=0$) or roughened ($\alpha\simeq0.5$) side surface, $l/D>5$.	$l_{eff}=D\left(\frac{2}{3}+\frac{\alpha}{1+\alpha}\right)$.

Remark: α – fraction of radiation which is isotropically scattered backward from the inside surface of the sample.

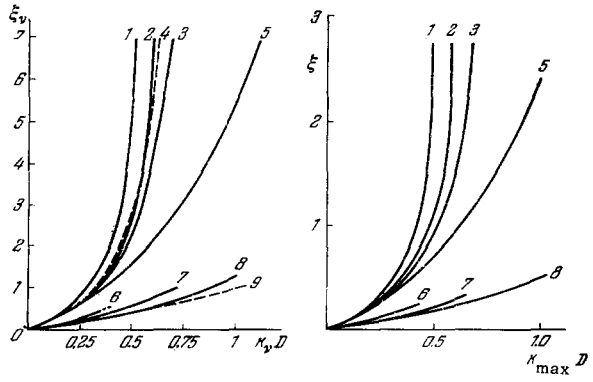

FIG. 2. Side surface roughened: 1,2,3 – according to [33], l/D is respectively 20, 10, and 5; 4 – according to (21). Immersion envelope: 5 – according to (20), $l/D = 10$, $D_0/D = \kappa = 1.5$. Polished side surface: 6,7,8 – according to [33], l/D respectively 20, 10, and 5; 9 – according to (20).

$\rho = 0$ and for a Lorentz line shape are shown in Fig. 2. We see that for small inversion the value of ξ is determined principally by the value of kD and depends little on the length of the sample. For roughened samples there are limits to the attainable inversion, determined by the condition $\alpha \exp[D(k - \rho)] = 1$ imposed by the required balance between the losses and the gain (see (21)).

With the aid of the foregoing relations and the data of Fig. 2 we can obtain, for the given excess over threshold n, the inversion and the gain in the medium. The obtained data show that in the stationary generation regime, when the average gain in the medium $k_{thr} = (\sigma + \ln 1/R)/2l$ is small (see (2')), the superluminescence is negligible when the rod dimensions are not too large. In addition to the amplification of the spontaneous emission, amplification of the pump radiation quanta with frequency ν_g is also possible. This effect is particularly significant when the medium has a broad amplification band. An estimate shows that in the case when neodymium glass is pumped by radiation from a xenon lamp with a brightness temperature $\sim 1.2 \times 10^4$ °K, the effect of the amplification of the pump radiation can become fully comparable with the superluminescence effect.

Monopulse regime [10,33,35-40]. Let us consider the case of instantaneous switching of the optical shutter (allowance for the finite switching time is made in [35,37,39], see Sec. III). At the instant of switching of the shutter, an inverted population N^0 is produced in the active rod, with a corresponding gain k_0 (see expressions (18) and (19)). Assuming that the following conditions are satisfied: 1) the duration T of the generation pulse is much larger than the time of flight in the resonator $\Delta t = [L + l(\kappa - 1)]/c$; 2) the gain is constant in the rod and the radiation-density distribution in the resonator does not differ greatly from the distribution in the case of the stationary regime; 3) the relaxation time of the lower working level (four-level medium) is much smaller than T, we can write the following equations for the four-level medium:

$$\frac{du_g}{dt} = \frac{l}{\Delta t}(k - k_1)u_g; \quad \frac{dN}{dt} = -NB_g u_g, \qquad (22)$$

where $k_{thr} = (1/2l)(\sigma + \sigma_{sh} + \ln 1/R)$; σ_{sh}—loss in the open shutter. It is seen from the first of these equations that the maximum radiation density is attained at an instant of time corresponding to $k = k_{thr}$.

In Table III we give expressions for the maximum pump power P in the pulse, the generation energy W, and the pulse duration T. We see that there exists an optimal mirror reflection coefficient R_0 for which the generation energy is maximal. The generation power P reaches a maximum at a somewhat different value of R [33].

It follows from (23)—(28) that in the case of large excess above threshold ($n_W \gg 1$ and $k_0 \gg k_{thr}$), it is possible to obtain very short pulses with large instantaneous power. An essential limitation of the attainable power and energy in the MP mode is the "collapse" of the excitation energy as a result of the superluminescence and the bleaching of the active medium when the ground level becomes depleted. Figure 3 shows by way of an example the calculated dependence of the maximum generation power on the excess over threshold (with respect to power) in the case of prolonged pumping [33]. We see that the influence of the superluminescence is quite significant for four-level media; in a three-level medium, the influence of bleaching is greater.

Amplification regime. This regime is of particular interest in the case of amplification of the power of monopulse and continuous lasers. The amplification of the stationary signal is considered in [22-28] and that of a pulse signal in [41-46]. A regenerative amplification regime, in which positive feedback is produced in the amplifier is considered in [41,13,47-49].

Let us consider the energy relations in the amplification regime in the absence of feedback in the

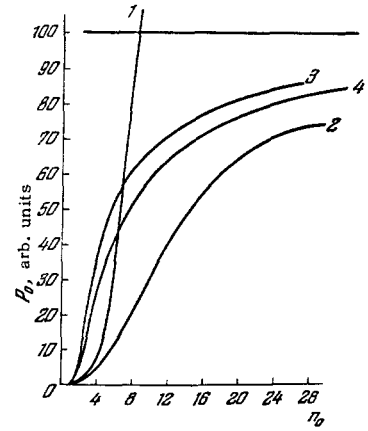

FIG. 3. $l = 8$ cm; L = 40 cm; D = 0.8 cm; $k_{thr_0} = 0.1$ cm^{-1}. 1 and 2 – four-level scheme $(N_0/\delta)|_{R=1} = 2 \times 10^2$; 3 and 4 – three-level scheme $(N_0/\delta)|_{R=1} = 4$; 1 and 3 – without allowance for the shortening of τ, 2 and 4 – with allowance.

Table III

Four-level medium	Three-level medium
$P=\frac{E\ln 1/R}{2\Delta t}\left[1-\frac{k_{thr}}{k_0}\left(1+\ln\frac{k_0}{k_{thr}}\right)\right]\simeq$	$P=\frac{E\ln 1/R}{4\Delta t}\left[1-\frac{k_{thr}}{k_0}\left(1+\ln\frac{k_0}{k_{thr}}\right)\right];$ (28)
$\simeq$ (for $t_{pul}\ll\tau_{eff}$) $\simeq\eta_1\frac{v_g}{v_p}\frac{\ln 1/R}{2\Delta t}\times$	$W=\frac{E\ln 1/R}{4lk_{thr}}\left(1-\frac{k_1}{k_0}\right)\simeq$
$\times W_p\left[1-\frac{1}{n_W}(1+\ln n_W)\right];$ (23)	$\simeq\left(\text{for }\frac{k_0}{k_{thr}}>1{,}05\right)\simeq$
$W=\frac{E\ln 1/R}{2lk_{thr}}\left(1-\frac{k_1}{k_0}\right)\simeq$	$\simeq\frac{E\ln 1/R}{4lk_{thr}}\left[1-\left(\frac{k_{thr}}{k_0}\right)^2\right];$ (29)
$\simeq\left(\text{for }\frac{k_0}{k_{thr}}>1{,}05\right)\simeq\frac{E\ln 1/R}{2lk_{thr}}\times$	
$\times\left[1-\left(\frac{k_{thr}}{k_0}\right)^2\right]\simeq$ (for $t_{pul}\ll\tau_{eff}$) $\simeq$	
$\simeq\eta_l\frac{v_g}{v_p}\frac{\ln 1/R}{\sigma+\sigma_{sh}+\ln 1/R}\times$	
$\times W_p\left(1-\frac{1}{n_W^2}\right);$ (24)	
$T\simeq\frac{W}{P}=\frac{\Delta t\,(1-k_1/k_0)}{lk_{thr}\left[1-\frac{k_{thr}}{k_0}\left(1+\ln\frac{k_0}{k_{thr}}\right)\right]}\simeq$	
$\simeq\left(\text{for }\frac{k_0}{k_{thr}}>1{,}05,\ t_{pul}\ll\tau_{eff}\right)\simeq$	
$\simeq\frac{\Delta t}{k_{thr}l}\frac{1-1/n_W^2}{1-\frac{1}{n_W}(1+\ln n_W)};$ (25)	
Optimal mirror reflection coefficient	
$W_0\Big\vert_{\frac{k_0}{k_{thr}}>1{,}05}\simeq E\left[1-\left(\frac{k_{thr}}{k_0}\right)^{2/3}\right]^2\simeq$	$W_0\simeq\frac{E}{2}\left[1-\left(\frac{k_{thr}}{k_0}\right)^{2/3}\right]^2.$ (30)
$\simeq$ (for $t_u\ll\tau_{eff}$) $\simeq$	
$\simeq\eta_l\frac{v_g}{v_p}W_p\ (1-n_{W_0}^{-2/3})^2;$ (26)	
$\ln 1/R_0\simeq 1{,}6k_{thr_0}l\left[\left(\frac{k_0}{k_{thr}}\right)^{2/3}_0-1\right];$ (27)	

Remark. k_1 – gain in the medium at the instant of the cessation of generation: $(k_0 - k_1)/k_{thr} = \ln k_0/k_1$. When $k_0/k_{thr} > 1.05$: $1 - k_1/k_0 \simeq 1 - (k_{thr}/k_0)^2 \cdot E = h\nu_g S l N^0 = c l S \Delta\nu_{1um} k_0/\kappa B_g$ – excitation energy stored in the sample. $k_{thr_0} = (1/2l)(\sigma + \sigma_3)n_{W_0}$ – excess over threshold pump energy when R = 1.

amplifier. For an amplifier using a four-level medium we can write the following equations:

$$\frac{\partial u_g}{\partial x}+\frac{\varkappa}{c}\frac{\partial u_g}{\partial t}=(k-\rho_0)u_g;$$
$$\frac{\partial N}{\partial t}=-NB_g u_g,$$

where ρ_0 is the loss per unit length of the active rod in the amplification regime, equal to the loss to the inactive absorption and scattering through large angles; usually $\rho_0 < \sigma/2l$ [28]. For a three-level medium, the equations are the same but a factor 2 appears in the right side of the second eqution. Going over from the radiation density u_g to the radiation energy $W_g = (c/\kappa)\Delta\nu_{lum}S\int_0^{t_{pul}} u_g dt$, we get [13]

$$\frac{dW_g}{dx}=\frac{E}{l}\left(1-e^{-\frac{\Lambda}{h\nu_g S}W_g}\right)-\rho_0 W_g, \qquad (31)$$

where $\Lambda = k/N$ is the cross section for induced transitions; a definition of E is given in Table III. Solutions of (31) are listed in Table IV [13].

In the presence of losses in the medium, there is a certain limiting value of the energy $W_{g.lim}$, at which the amplification and the losses compensate

Table IV

Regime	Four-level medium	Three-level medium
Amplification of short pulse	1) $\rho_0 = 0$. $W_g = W_0 + E + \frac{h\nu_g S}{\Lambda} \ln\left\{1 - \exp\times\right.$ $\left.\times\left[-\frac{\Lambda}{h\nu_g S} W_0 (1 - e^{-\frac{\Lambda}{h\nu_g S}E})\right]\right\}$. For a strong input signal $\left(\frac{\Lambda}{h\nu_g S} W_0 \gg 1\right)$ $W_g \simeq W_0 + E$. 2) Weak input signal $\frac{\Lambda}{h\nu_g S} W_g \ll 1$, $W_g = W_0 \exp\left(\frac{\Lambda}{h\nu_g S} E - \rho_0 l\right)$.	1) $\rho_0 = 0$. $W_g = W_0 + \frac{1}{2}E + \frac{h\nu_g S}{2\Lambda} \ln\left\{1 - \exp\times\right.$ $\left.\times\left[-\frac{2\Lambda}{h\nu_g S} W_0 (1 - e^{-\frac{\Lambda}{h\nu_g S}E})\right]\right\}$. 2) $\frac{2\Lambda}{h\nu_g S} W_g \ll 1$, $W_g = W_0 \exp\left(\frac{\Lambda}{h\nu_g S} E - \rho_0 l\right)$.
Amplification of stationary signal	$\ln \frac{P_g}{P_0} = (k_0 - \rho_0) l + \frac{k_0}{\rho_0} \ln\left[1 - \frac{\frac{P_g}{P_0} - 1}{\frac{k_0}{\rho_0} - 1}\right]$.	

Note. $W_g(P_g)$ – energy (power) of signal at the amplifier output. $W_0(P_0)$ – the same at the amplifier input; k_0 – gain in the medium in the absence of an amplified signal; $u(0) = \kappa P_0 / c\Delta\nu_{lum} S$ – density of amplified radiation at the amplifier input.

each other and the pulse energy ceases to grow with increasing rod length. From (31) with $dW_g/dx = 0$ and $\rho_0 \ll \Lambda E/h\nu_g S l$ it follows [13] that $W_{g.lim} \simeq E/\rho_0 l$.

The temporal characteristics of the amplified pulse were considered in [42,43,13,45,46,275]. In particular, it is shown in [45,46] that if the leading front of the amplified pulse is exponential, the duration of the pulse in the amplifier does not change, but a for a rectangular or Gaussian front the pulse becomes shorter [275].

The connection between input and output signals of the amplifier, in the stationary case, is shown in Table IV [28]. It is easy to verify that an increase in the value of the input signal leads to a decrease in the value of the gain, the gain being P_g/P_0. The stationary amplification regime in the case of an inhomogeneously broadened line is considered in [276].

Features of laser calculations. In the calculation of the threshold pump intensity and the laser generation intensity, it is necessary to take into account the presence of several absorption bands of the active medium, the radiation energy yield of the pump source, and the efficiency and uneven distribution of the pump power over the cross section of the illuminator rod. By way of an example we present an expression for the threshold and generation power of a laser operating in the stationary regime with a four-level medium [26,50]:

$$P_{e,thr} = \frac{4\pi h \varkappa^2 \gamma S \nu_g^2 \Delta\nu_{lum} (\sigma + \ln 1/R)}{\omega \sum_i \eta_i \theta_i F_i / \nu_{pi}}; \qquad (7')$$

$$P_g = \omega \nu_g \frac{\ln 1/R}{\sigma + \ln 1/R} \left(P_e - \frac{P_{e,thr}}{\gamma}\right) \sum_i \eta_{1i} \theta_i F_i / \nu_{p_i}, \qquad (9')$$

where P_e—electric power fed to the pump lamp ($P_{e.thr}$ is the corresponding threshold power); ω—efficiency of illuminator; γ—coefficient of uniformity of the pumping (for a definition of ω and γ see Sec. III, 3b); θ_i—fraction of pump radiation incident on the rod in the i-th pump band and absorbed by the rod; F_i—energy yield of the pump-source radiation in the i-th band (in (9′) it is assumed that the entire end surface of the rod generates).

2. Multi-mode Generation

When considering multi-mode generation it is necessary to take into account the spatial distribution of the individual modes, as was demonstrated, in particular, in [51]; the method of calculating multi-mode generation was developed by Tang and Statz [5,6] and was further developed in [52–54,14–16].

Let us consider the stationary regime of a laser with a flat ribbon resonator (mirrors in the form of

infinite strips of width D); we shall describe the active medium with the aid of equations of the type (2) and (3) (two-level model). It is assumed that the luminescence line has a Lorentz contour and is uniformly broadened. For a four-level medium, the population balance equation is written in the form

$$\eta_1 B_p u_p N_0 - \frac{N}{\tau} - \frac{B_r N}{\frac{\pi}{2}\Delta\nu_{lum}} \sum_{i,j} u_{ij}\varphi_i(z)\psi_j(x) g_{ij} = 0, \quad (32)$$

where i and j are the axial and angular mode indices; u_{ij}—average radiation power in the mode with indices i and j;

$$\varphi_i(z) = 2\sin^2\frac{\pi i}{L}z = 1 - \cos\frac{2\pi i}{L}z \text{ и } \psi_j(x) = 1 - \cos\frac{2\pi j}{D}x$$

—mode radiation density distribution functions in the axial and transverse directions of the resonator ($0 \le z \le L$; $0 \le x \le D$); $g_{ij} \simeq g_i = [1 + (2\nu_i - \nu_0/\Delta\nu_{lum})^2]^{-1}$ – relative intensity of the luminescence line at the frequency ν_i (the mode radiation frequency ν_{ij} depends principally on the axial index i); ν_0—frequency corresponding to the center of the luminescence line. The pump distribution is assumed uniform. The summation in (32) is over all the excited modes.

The balance equations for the radiation density of the modes, u_{ij}, similar to (22), is written in the form

$$-\frac{cD\sigma_{ij}}{2\varkappa h\nu_g}u_{ij} + \frac{B_g g_i u_{ij}}{\frac{\pi}{2}\Delta\nu_{lum}}\int_0^L\int_0^D N\varphi_i(z)\psi_j(x)\,dz\,dx = 0, \quad (33)$$

where $\sigma_{ij} \equiv \sigma_j = \sigma_0 + \sigma_j^d$—loss for mode with angular index j (the loss does not depend on the index i; see Sec. III); $\sigma_0 \simeq \ln 1/R$—nonselective losses; σ_j^d—diffraction losses.

From (32) and (33) we can readily obtain

$$\frac{ng_i}{LD}\int_0^L\int_0^D \frac{\varphi_i\psi_j\,dz\,dx}{1+\sum_{i,j}A_{ij}\varphi_i\psi_j} = \frac{\sigma_j}{\sigma_1}, \quad (34)$$

where σ_1—loss for the lower mode and n—excess above threshold; $A_{ij} \equiv \frac{B_g\tau}{\frac{\pi}{2}\Delta\nu_{lum}}u_{ij}$. The solution of a system of the type (34) with respect to A_{ij} is a rather complicated task. However, as shown in [6,15], when the number of excited modes is large it is possible to solve independently, with sufficiently good approximation, the problem of the distribution of radiation with respect to the axial and angular modes. In this case the equations for the axial modes, analogous to (34), are

$$\frac{n}{L}\int_0^L \frac{\varphi_i\,dz}{1+\sum_i A_i\varphi_i} = \frac{1}{g_i}, \quad (34')$$

and for transverse modes

$$\frac{n}{D}\int_0^D \frac{\psi_j\,dx}{1+\sum_j A_j'\psi_j} = \frac{\sigma_j}{\sigma_1}. \quad (34'')$$

A_i is proportional to the total radiation density of the modes with identical axial index i and different angular indices, while A_j' is proportional to the corresponding density of the modes with identical transverse index and different axial indices.

Using the expansion [52,53]

$$\left(1+\sum_i A_i\varphi_i\right)^{-1} \simeq \frac{1}{1+\sum_i A_i}\left[1 + \frac{\sum_i A_i\cos\frac{2\pi i}{L}z}{1+\sum_i A_i}\right],$$

we can reduce (34′) to the form

$$n\left[\frac{1}{1+\sum_i A_i} - \frac{1}{2}\frac{A_i}{(1+\sum_i A_i)^2}\right] = \frac{1}{g_i}. \quad (35)$$

Recognizing that for modes that are not excited under the given conditions the left side of (35) is smaller than the right side, we can easily solve a system of the type (35) for all the excited axial modes with respect to A_i [52,53,14]. It follows from the solution that the total number q of the excited modes with different axial indices is given by the relation [14]

$$q \simeq \left(\frac{\Delta\nu_{lum}}{\delta\nu}\right)^{2/3}\left(\frac{n-1}{n}\right)^{1/3}, \quad (36')$$

where $\delta\nu = c/2\varkappa L$ is the distance between neighboring axial modes (see Sec. III). Since the total width of the generation spectrum is $\Delta\nu_g \simeq q\,\delta\nu$, we can write (36′) in the form

$$\Delta\nu_g \simeq \Delta\nu_{lum}^{2/3}\delta\nu^{1/3}\left(\frac{n-1}{n}\right)^{1/3}. \quad (36)$$

The half-width of the spectrum at half the maximum amplitude is, according to [53], $0.7\,\Delta\nu_g$. It follows from (36) that the width of the generation spectrum reaches saturation rapidly with increasing excess over threshold n.

For a three-level active medium, the expression for $\Delta\nu_g$ takes the form (36), but corresponding to the value of n in this case is $(P_p - P_0)(P_{thr} + P_0)/(P_p + P_0)(P_{thr} - P_0)$, where P_0 is the pump power at which $N = 0$. We note that the relation obtained for $\Delta\nu_g$ does not depend on the configuration of the plane resonator mirrors.

It is shown in [54,14] that the diffusion of excitation in the active medium of solid-state lasers has practically no effect on the width of the generation spectrum. At low temperatures, an important role is played in a number of media by the inhomogeneous line-broadening mechanism (see Sec. III), wherein the width of the generation spectrum may turn out to be much larger than that given by (36).

It is possible to solve similarly the system (34″) for the angular modess [6,15,16]. Recognizing that $\sigma_j^d \simeq j^2\sigma_1^d \simeq j^2\cdot 2(\sqrt{\lambda L/D})^3$ for a ribbon resonator [4], Eq. (34″) yields, for $\sigma_1^d \ll \sigma_0$, the following expression for the number of observed angular modes, m ($m \ge 3$), and for the generation power P_g [15,16]:

$$\frac{4}{3}m^3 + 2m^2 \approx \frac{\sigma_0}{\sigma_1^p}\left(1 - \frac{1}{n}\right);$$

$$P_g \simeq \frac{m-\frac{1}{2}}{m}\frac{\sigma_0}{\sigma_0+\overline{\sigma^d}}\eta_1\frac{\nu_g}{\nu_p}P_p\left(1 - \frac{m}{m-\frac{1}{2}}\frac{\sigma_0+\overline{\sigma^d}}{\sigma_0}\frac{1}{n}\right)$$

$$\approx \eta_1\frac{\nu_g}{\nu_p}P_p\frac{\sigma_0}{\sigma_0+\overline{\sigma^d}}\left(1 - \frac{\sigma_0+\overline{\sigma^d}}{\sigma_0}\frac{1}{n}\right), \quad (37)$$

where $\overline{\sigma^d} = (1/m)\sum_1^m \sigma_j^d$ is the average diffraction loss for m excited modes. Expression (37) is valid also for the case of a three-level medium, with allowance for the remark made concerning the value of n in relation (36) for a three-level medium.

The angular divergence of the laser emission (along the x axis) is $m\alpha_d$, where $\alpha_d \simeq \lambda/D$ (see Sec. III). It follows from (37) that the angular divergence saturates quite rapidly with increasing pump, reaching a limiting value

$$\alpha_{lim} \approx 0{,}7\sigma_0^{1/3}\left(\frac{\lambda}{L}\right)^{1/2} \quad (39)$$

at a threshold ratio $n > 2$.

For a resonator with square mirrors measuring $D \times D$, the angular divergence in each of two mutually perpendicular directions is quite close to the values given by relation (37) or (39)[15]. Expression (36) for the generation power also remains in force, but the averaging of σ^d must be carried out over all the excited modes. It can be assumed that the obtained relations are effective also for a resonator with round mirrors of diameter D. Within the framework of the given model, we can also take into account the effect of the uneven pump distribution on the angular divergence [15].

The foregoing results show that the method of kinetic equations makes it possible to study the energy, spectral, and angular parameters of a laser. Naturally, the results obtained by this method are approximate and call for at least an experimental confirmation. The most essential effect which cannot be accounted for in the employed model is apparently the excitation of coupled modes, especially in the presence of scattering in the active medium. In this case, the angular divergence of the radiation greatly exceeds the value given by (39) (see, for example, [16] and Sec. IV). The energies of the generation process can also be greatly influenced by the interaction between modes having close frequencies [8].

The kinetics of the monopulse operation is considered in [228] with allowance for the spatial and frequency characteristics of the angular modes of the resonator. It is shown that, owing to the unavoidable inhomogeneity of the initial distribution of the inversion over the cross section of the rod, different zones of the cross section take part in the generation during different stages of the development of the giant pulse, leading to a lengthening of the summary generation pulse and to a time variation of the radiation divergence angle.

III. LASER ELEMENTS

1. Active Media

The number of presently known active media is large. A most complete table of the active media developed to date on the basis of inorganic materials with ionic structure, as well as information on their crystal-chemical structure and growth technology, is contained in [55,56]. In this review we consider only a small number of media that have found practical application.

The presented analysis of laser operation enables us to formulate certain requirements that active media must satisfy. These include requirements such as the presence of a narrow luminescence line of the working transition and broad intense absorption bands, a large luminescence quantum yield and a large yield of excitation of the upper working level, small Stokes losses, absence of absorption from the upper working level to higher levels, especially at the frequency of the working transition, a large energy gap between the ground and lower working level (for four-level media), small losses and optical homogeneity of the medium. These requirements are common to all laser operating regimes. The value of the lifetime τ affects the laser characteristics in a complicated manner. In the pulsed regime, a decrease of τ leads to a decrease in the threshold pump energy. In the continuous regime, for four-level media (with quenched lower level) τ has no influence on the threshold, and for three-level media an increase in τ leads to a decrease of the threshold, so long as $\delta/N_0 \ll 1$. In the case of the monopulse regime, an increase of τ makes it possible to increase the accumulated excitation energy, but the threshold is raised thereby.

Another very complicated question is that of the influence of the activator concentration on the laser parameters. On the one hand, an increase in the concentration increases the intensity of the absorption bands of the medium; on the other, starting with certain concentration values, concentration quenching of the luminescence occurs and decreases τ and the quantum yield [57,26], and also affects adversely the optical quality of the material [58]. The optimal activator concentration is usually chosen experimentally. Figure 4 shows the dependence of the characteristics of a $CaWO_4:Nd^{3+}$ laser [58] and a neodymium-glass laser [26] on the Nd^{3+} ion concentration. Figure 4a shows also the glass-laser parameters as calculated from (9) and (15).

The activators employed are divalent and trivalent rare-earth ions (Nd^{3+}, Sm^{2+}, Dy^{2+}), actinide ions (U^{3+}), and ions of transition-group elements (Cr^{3+}), in which the luminescence lines are quite narrow be-

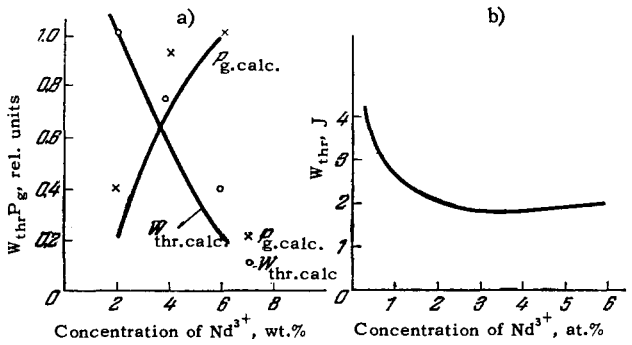

FIG. 4. a – neodymium glass; b – $CaWO_4:Nd^{3+}$.

cause the optical transitions occur within internal well-screened shells.

Of greatest interest at present are the following active media: ruby ($Al_2O_3:Cr^{3+}$), glass activated with trivalent neodymium ions, $CaWO_4$; Nd^{3+} [59], $YAlG:Nd^{3+}$ [60-62], $CaF_2:Dy^{2+}$ [63-66], and $CaF_2:Sm^{2+}$ [67]. The lower-level schemes and the luminescence and absorption spectra of Cr^{3+} in ruby [68,69] and Nd^{3+} in glass [70,71] are shown in Fig. 5.

We see that ruby is a three-level medium and neodymium-glass a four-level medium. The spacing between the lower working and ground levels in the Nd^{3+} ions is ~2000 cm^{-1}, so that the lower level of this ion is sufficiently quenched even at room temperature. The principal generating lines are the line R_1 (λ = 6943 Å) in ruby and the line with λ = 10 600 Å in neodymium glass. The ^2E level of the Cr^{3+} ion in ruby is split into two sublevels, spaced 29 cm^{-1} apart and corresponding to the R_1 and R_2 luminescence lines. The time of spectral relaxation between these sublevels is less than 10^{-7} sec. The absorption spectra of excited levels were investigated in [72-74], where the presence of intense absorption from the metastable level ^2E to higher levels has been established; the bands of this absorption overlap the bands of absorption from the ground level $^4A_2$ ($\lambda \cong$ 560, 450, 360, and 260 nm). At the same time, rapid nonradiative relaxation from the higher levels back to the ^2E level takes place, with efficiency ~90% [73,74]. Thus, the presence of absorption from the upper working level causes a considerable fraction (~50%) of the absorbed pump radiation to be transformed into heat dissipated in the crystal.

Table V lists the main spectral characteristics of a number of active media. One of the most promising possibilities of effective control of the characteristics of an active medium is to vary the crystal or vitreous structure into which the activator ions are introduced [75-77]. The data listed in Table V illustrate, with Nd^{3+} as the example, the effect of the matrix on the characteristics of the active medium. The results of [76-78] show, in particular, that by varying the composition of the glass it is possible to control the value of τ of Nd^{3+} within a range 30—1000 μsec, without essentially varying the luminescence quantum yield.

In the case of heterovalent penetration of the activator into the matrix, luminescence centers with different surrounding-field symmetries can be produced [56,79]. The spectral characteristics of the activator ion change appreciably with change in the structure of the center, as is observed, for example, when CaF_2 crystals are activated with U^{3+} ions [80,81]

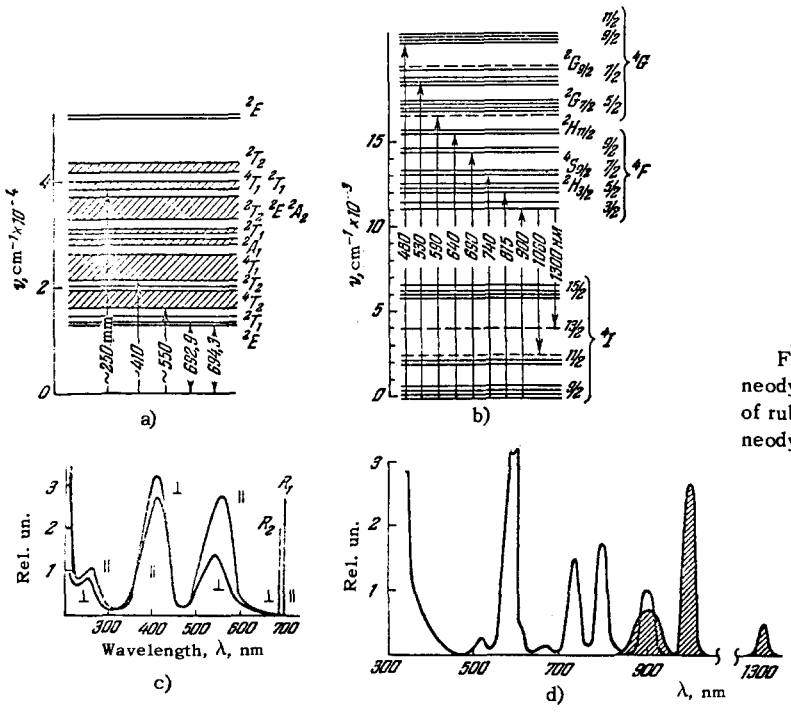

FIG. 5. a – level scheme of ruby; b – level scheme of neodymium glass; c – absorption and luminescence spectra of ruby; d – absorption and luminescence (shaded) spectra of neodymium glass.

Table V

Medium	Activator concentration, %	Main absorption bands, μ	Half-width of absorption bands,* A	Luminescence quantum yield,** %	η_1, %	λ_2, μ	Luminescence line half-width, A	τ, μ sec	Note
Ruby	0,03—0,05 (mol)	0,55 0,4	550 700	70 70	70 70	0,6943	5,5	$3\cdot10^3$	$T = 300°$ K 68, 69, 84, 85
Neodym. glass	2 (wt)	0,88 0,81 0,74 0,58	250 300 300 300	30 23 10 10	100 77 33 33	1,06	220	670	$T = 300°$ K 26, 71, 86
	6 (wt)	0,88 0,81 0,74 0,58	250 300 300 300	21 13 7 5	100 62 31 25	1,06	220	440	
$CaWO_4 : Nd^{3+}$	2 (mol)	0,88 0,81 0,74 0,58	100 200 200 200	36 28 14 10	100 78 39 28	1,058	50	160	$T = 300°$ K 26, 87, 88
$YAlG : Nd^{3+}$	3 (mol)	0,88 0,82 0,76 0,585	~150 ~200 ~230 ~150			1,0648	6,5	180	$T = 300°$ K 60, 62, 87, 89
$CaF_2 : Dy^{2+}$	0,02 (mol)	0,9 0,7 0,55	850 680 1000	3 — 12	~20	2,358	1,2	$\sim 15\cdot10^3$	$T = 77°$ K 26, 66, 88
$CaF_2 : Sm^{2+}$	0,02 (mol)	0,63 0,42	480 180	~10	100 (?)	0,708	0,8—1	1—2	$T = 20°$ K 67

*In the case of structured absorption bands ($CaWO_4:Nd^{3+}$, $YAlG:Nd^{3+}$), the equivalent band widths are presented.

**The luminescence quantum yield presented is that corresponding to the working transition. For ruby, the summary quantum yield for the R lines is given.

or CaF_2 and $CaWO_4$ crystals are activated with Nd^{3+} ions [55, 82, 83]. The influence of the structure of the centers on the generation spectrum of these media is considered in Sec. IV.

An important factor which determines to a considerable degree the laser emission spectrum is the character of the luminescence line broadening in the active medium. The main causes of line broadening in crystals and glasses are electron-vibrational interactions in the lattice and the presence of inhomogeneities in the structure of the material [90-92, 143]. The first factor causes homogeneous broadening of the line, and the second inhomogeneous broadening. As a rule, in homogeneous broadening the line has a Lorentz contour and the line width and shift have a strong temperature dependence; in inhomogeneous broadening one can expect a Gaussian distribution of the intensity in the line and a weak dependence of the line width on the temperature [143]. Figure 6 shows plots of the luminescence line widths against the temperature for a number of media. In ruby at T > 100°K there is apparently homogeneous line broadening, as confirmed by a study of the line contour [90] and generation spectrum in a traveling-wave laser [93]. A similar character of the broadening was observed in $CaF_2 : Sm^{2+}$ [52, 94] and $CaF_2 : U^{3+}$ (T > 50°K) [95].

An investigation of the luminescence and generation spectrum [95, 96] led to the conclusion that the line broadening in $CaF_2 : Dy^{2+}$ crystals is inhomogeneous. However, a theoretical estimate of the lifetime of the lower working level [277] favors the conclusion of a homogeneous line broadening in these crystals. The question of the character of the line broadening in neodymium glass still remains unanswered. Some data on the structure of the generation spectrum of neodymium glasses [97, 98, 278, 279], as well as the absence of a fine structure in the luminescence spec-

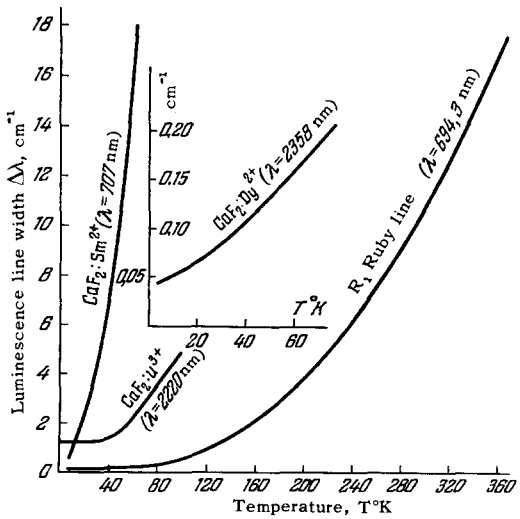

FIG. 6.

Table VI

Base	Activator	Sensitizer	Excitation-transfer mechanism	Effect given by the sensitization	Reference
YAlG	Nd^{3+}	Cr^{3+}	Resonance	Threshold decreases approximately by a factor of 2, the efficiency is tripled.	61
ErYAlG	Ho^{3+}	Основа	Resonance	The luminescence increases 20 times. The threshold is 47 W when an incandescent lamp is used for pumping (T = 77°K).	100
Glass	Nd^{3+}	Mn^{2+}	Resonance		101, 102
Glass	Nd^{3+}	Ce^{3+}	Reabsorption	Radiation intensity increases 50%.	103

trum even at low temperatures [70], give grounds for assuming that line broadening in neodymium glass is inhomogeneous. However, experiments on the dynamics of the emission within the luminescence bands, in which short-duration generation pulses were applied to the neodymium glass, has shown that the time of spectral relaxation in the luminescence band of neodymium glass is quite short and does not exceed 10^{-6}—10^{-8} sec [96,99].

Considerable interest attaches to excitation-energy transport in the active media and the related question of sensitization of the luminescence of the activator. Sensitization of the activator-ion emission makes it possible to broaden the effective absorption band of the pump radiation and by the same token increase the laser efficiency. The sensitizer may be an additive introduced into the lattice, as well as the crystal base, and in the latter case the efficiency of the sensitization may be appreciable, owing to the large width of the lattice absorption bands. The possible mechanisms whereby excitation energy is transferred from the sensitizer to the activator are resonant excitation transfer and reabsorption of radiation.

Table VI lists a number of active media in which sensitization is used.

The excitation-migration processes can play a certain role in the formation of the generation spectrum, since they influence the spatial distribution of the inversion in the medium [5,54]. In the case of homogeneous broadening of the luminescence line, in the presence of inversion in the medium, deactivation by stimulated emission of centers with overlapping luminescence bands can cause a rapid "mixing" of the excitation energy of different centers (see the foregoing discussion of the relaxation time in glass) and lead to a number of unique effects in the generation spectrum. Such effects are observed, for example, in lasers based on $CaF_2:U^{3+}$ containing two types of centers with overlapping luminescence bands [81]; it is possible that they should be taken into account in the interpretation of the neodymium-glass generation spectra.

In addition to the spectral characteristics of the active materials, importance attaches to such properties as optical homogeneity, magnitude of the losses (which affects the Q of the resonator), thermophysical parameters (which govern the thermal deformation of the active medium), thermal endurance of the materials, etc. The characteristics of a number of active media are listed in Table VII. The material which is most perfect optically is neodymium glass, since it has very small optical scattering and high homogeneity. Shortcomings of glass are low thermal conductivity and thermal endurance. Fluorite is optically homogeneous, but the light scattering in it is appreciable [16]. Such materials as ruby and yttrium aluminum garnet have high thermal endurance, but their optical homogeneity is relatively low.

Table VII

Material	Density, g/cm³	Refractive index	$\frac{d\varkappa}{dT}$, deg^{-1}	Specific heat, cal/g-deg	Thermal conductivity coefficient, cal/deg-cm-sec	Coefficient of thermal expansion, deg^{-1}	Coefficient of inactive absorption, cm^{-1}	Scattering coefficient, cm^{-1}
Ruby	3.98	1.76	$(1{,}26-1{,}75)\cdot10^{-5}$	0.1813	0,06— $\parallel c$ -axis 0.055— $\perp c$ -axis	$6.6\cdot10^{-6}$ — $\parallel c$ -axis $5\cdot10^{-6}$ — $\perp c$ -axis		0,02 — 0,1 [104]
Neodymium glass	2.95	1.55	$2\cdot10^{-6}$	0.16	0,0016	$1.1\cdot10^{-5}$	$1{,}5\cdot10^{-3}$ [105]	$<0{,}004$ [105]
$CaWO_4:Nd^{3+}$	6.06	1.92		0.104	0.0079— $\parallel c$ -axis	$11{,}2\cdot10^{-6}$ — $\parallel \alpha$ -axis $18.7\cdot10^{-6}$ $\perp c$ -axis		
$CaF_2:Sm^{2+}$	3.18	1.435		0.21	0,093 (83° K) 0.02 (300° K)	$18.4\cdot10^{-6}$		0,02 — 0,04 [16]

Note: Unless otherwise stipulated, all data are for T = 300°K.

Table VIII

Resonator	Spectral distance between modes, $\Delta\nu$, cm^{-1}	Diffraction losses σ_d (for two passes)	Angular mode divergence α, rad	Distribution of field amplitude
Planar	$\frac{\Delta q}{2L}+\frac{\lambda}{4D^2}(m\,\Delta m+n\,\Delta n)$ $m,\ n=1,\ 2,\ 3\ \ldots$	$2\left(\frac{\sqrt{L\lambda}}{D}\right)^3(m^2+n^2)$	$\frac{\lambda}{D}\sqrt{m^2+n^2}$	$\sin\frac{\pi m}{D}\left(x-\frac{D}{2}\right)\cdot\sin\frac{\pi n}{D}\left(y-\frac{D}{2}\right)$
Confocal r = L	$\frac{\Delta q}{2L}+\frac{\Delta(m+n)}{4L}$ $m,\ n=0,\ 1,\ 2\ \ldots$		$2\sqrt{\frac{\lambda}{\pi l}}\ \varkappa_m=\frac{2\varkappa_m^2}{\pi}\frac{\lambda}{d}$	$H_m\left(2x\sqrt{\frac{\pi}{L\lambda\left[1+\left(\frac{2z}{L}\right)^2\right]}}\right)\times$ $\times H_n\left(2x\sqrt{\frac{\pi}{L\lambda\left[1+\left(\frac{2z}{L}\right)^2\right]}}\right)\times$ $\times\exp\left\{-\frac{2\pi(x^2+y^2)}{L\lambda\left[1+\left(\frac{2z}{L}\right)^2\right]}\right.$
Spherical r ≥ L/2	$\frac{\Delta q}{2L}+\frac{\Delta(m+n)}{4L}\times$ $\times\left(1-\frac{4}{\pi}\operatorname{arctg}\frac{L_{\text{eff}}-L}{L_{\text{eff}}+L}\right)$		$2\varkappa_m\sqrt{\frac{\lambda}{\pi L_{\text{eff}}}}=$ $=\frac{2\varkappa_m^2}{\pi}\frac{\lambda}{d}$	Similar to the distribution for a confocal resonator with L replaced by L_{eff}.

Note. H_m and H_n are Hermite polynomials; the z axis is directed along the resonator axis and the origin is half-way between the mirrors.

Interference patterns of treated ruby and neodymium glass are given in Fig. 11 below.

2. Resonators

The resonators customarily used in solid-state lasers have either flat or spherical mirrors. We present in this section the main results of diffraction theory of passive open symmetrical resonators, as developed in [2-4,107,300], although it should be borne in mind that introduction of the active medium into the resonator leads to a number of peculiarities in the laser operation (formation of coupled modes, mode pulling, etc.; Sec. IV).

The modes excited in the resonator can in general be characterized by three indices: axial q, characterizing the distribution of the mode field in the direction of the resonator axis, and two angular indices (transverse) m and n, characterizing the distribution of the mode field in a plane perpendicular to the resonator axis, as well as the divergence of the mode radiation. Modes having identical angular and different axial indices differ only in the radiation frequency. Since the resonator electromagnetic oscillations of interest are transverse, the modes are denote TEM_{qmn}. Resonators are characterized by two parameters: the number of Fresnel zones $N = D^2/4L\lambda$ and the parameter $G = 1 - L/r$, where r is the radius of curvature of the resonator mirrors, L is the resonator length, and D is the mirror dimension. In a plane resonator G = 1 and in a confocal resonator G = 0. Table VIII lists the main characteristics of the modes of resonators with quadratic mirrors (D—length of side of the square). The relations can be used for estimating purposes also in the case of resonators with round mirrors of diameter D (see [4]). It is seen that modes whose axial indices differ by unity ($\Delta q = 1$) are spaced by a distance $\Delta\nu_a = (\frac{1}{2}l)\ cm^{-1}$. For L = 10 cm we have $\Delta\nu_a = 5 \times 10^{-2}\ cm^{-1}$. The modes of a planar resonator with angular indices differing by unity (Δm or $\Delta n = 1$) are spaced $\Delta\nu_{ang} = (\lambda/4D^2)m\Delta m$ apart. For the two lowest modes ($m_1 = 1$; $m_2 = 2$), we have $\Delta\nu_{ang} \simeq 10^{-4}\ cm^{-1}$ for $\lambda = 10^{-4}$ cm and D = 1.0 cm. Thus, in a planar resonator $\Delta\nu_a \gg \Delta\nu_{ang}$. The angular divergence of the modes increases with increasing angular indices, and for the lowest mode of a planar resonator we have $\alpha \simeq \alpha_d \simeq \lambda/D$.

In a confocal resonator, the distribution of the mode field is described by Gauss-Hermite functions[3], and the equal-phase surfaces are spheres whose curvature centers are located on the resonator axis, including the resonator mirror. The field in such a resonator is concentrated towards the axis, and the dimension of the excited region in the symmetry plane perpendicular to the resonator axis and com-

Table IX

m	0	1	2	3	4	5	6	7	8	9	10	11	12	13	14
$\varkappa_m$	1.86	2.51	2.97	3.35	3.68	3.98	4.25	4.5	4.73	4.97	5.18	5.38	5.57	5.76	5.93

prising an equal-phase surface is (at a field intensity level equal to 0.03 of maximum)

$$d = \varkappa_m \sqrt{\frac{L\lambda}{\pi}}, \tag{40}$$

where L = r is the radius of curvature of the mirrors, and κ_m is a coefficient that depends on the angular mode index m(n). The values of κ_m are listed in Table IX [108].

When considering a spherical confocal resonator with mirror radius of curvature $r \geq L/2$, it is convenient to use the concept of an equivalent confocal resonator [3], in which the field distribution coincides with the distribution of the field in the given resonator. The distance between mirrors of an equivalent confocal resonator is determined by the relation

$$L_{\text{eff}}^2 = 2Lr - L^2.$$

The dimension of the excited region in the symmetry plane of a nonconfocal resonator can be obtained from expression (40), by substituting in it L_{eff} in lieu of L. For a given L, the magnitude of d is minimal for a confocal resonator. More details on the distribution of the field in the spherical resonator are given in [3,4], and the characteristics of a concentric resonator are considered in [109]. The spectrum of a confocal resonator is partially degenerate, the degenerate modes being spaced $\frac{1}{4}L$ apart. The degeneracy is lifted if the resonator is made nonconfocal. When $r \simeq L$ we have

$$\Delta\nu \simeq \frac{\Delta q}{2L} + \frac{\Lambda(m+n)}{4L}\left[1 - \frac{2}{\pi}\left(1 - \frac{r}{L}\right)\right].$$

The diffraction loss in a spherical resonator is smaller than in a planar resonator when $r > L/2$. The minimum loss takes place in a confocal resonator. The dependence of the diffraction loss on the factor G for the two lowest modes of a cylindrical ribbon resonator with mirror with D is shown in Fig. 7 [110].

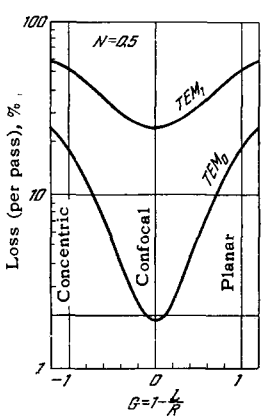

FIG. 7.

If a lens with focal length f is placed between the mirrors of a resonator, it becomes equivalent to a spherical resonator (Fig. 8). The parameters of the equivalent resonator can be obtained with the aid of the relations [111]

$$\left.\begin{aligned} L_1 &= l_1 + l_2 - \frac{l_1 l_2}{f}, \\ \frac{1}{R_1} &= \frac{1}{r_1} + \frac{l_2}{L_1 f}; \quad \frac{1}{R_2} = \frac{1}{r_2} + \frac{l_1}{L_1 f}. \end{aligned}\right\} \tag{41}$$

Real resonators of solid-state lasers deviate from ideal shape, owing to inaccuracies in the manufacture and adjustment of the elements, inhomogeneity of the active rod, and thermal deformation of the latter during pumping. The influence of defects of this kind is considered in [110,112,113,300]. It has been established that in the case of deviations from planarity of the resonator mirrors, the modes become deformed, and the angular divergence of the radiation as well as the spectral spacings $\Delta\nu_{\text{ang}}$ increase. The dependence of the diffraction losses on the mirror misalignment angle is shown in Fig. 9 for a planar resonator.

The criterion for the applicability of the theory of a planar resonator can be written in the form [108,113,114]

$$\frac{\Delta L}{\lambda} < \frac{1}{N}, \tag{42}$$

where ΔL is the maximum difference of the optical path in the resonator and N is the number of Fresnel zones. Since $N \simeq 10$—100 in solid-state lasers, the theory is applicable for deviations from planarity $\Delta L < (0.1$—$0.001)\lambda$.

The region of applicability of the theory of the spherical resonator is determined from the condition that the dimension of the spot on the mirror be

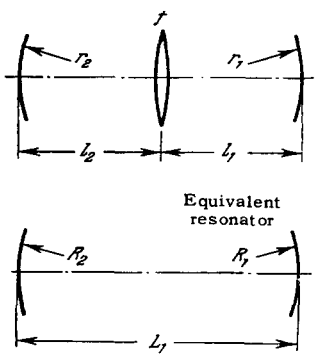

FIG. 8.

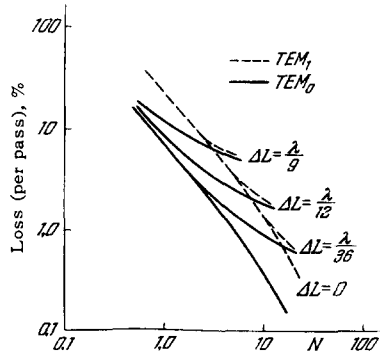

FIG. 9. Dependence of diffraction losses in a ribbon resonator with mirror width D on the mirror misalignment angle $\Delta\varphi = \Delta L/D$.

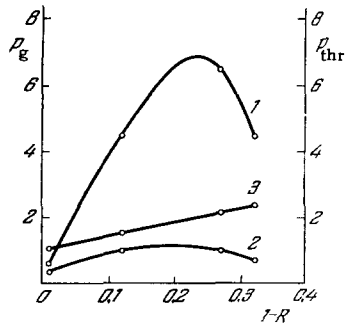

FIG. 10. Generation intensity P_g and threshold pump intensity P_{thr} vs. mirror reflection coefficient ($CaF_2:U^{3+}$, T = 78°K). Curves 1 and 2 – P_g (1 – threshold ratio n = 10, 2 – n = 6.7), 3 – P_{thr}.

smaller than the dimension of the mirror; this condition can be written in the form

$$\frac{\Delta L}{\lambda} > \frac{1}{2\pi^2 N}.$$

As a rule, this condition is always satisfied, and in the case of axially-symmetrical resonator deformation one can use for a rough estimate of the mode parameters (for example, angular divergence) the theory of the spherical resonator [108]. In particular, it follows from this that when condition (42) is satisfied the relative broadening of the angular divergence of the lowest mode of a planar resonator does not exceed ~2.

The characteristics of the resonator modes may be greatly influenced by an uneven distribution of the pump over the cross section of the active rod. It is shown in [115,116] that in the case of non-uniform inversion the radiation energy "spreads out" from the region of large inversion to the region of small inversion, thus causing deformation of the modes. The effect of inversion saturation in multimode generation on the excited modes is considered in [117,15].

Besides the near-axis modes considered above, total internal reflection from the side walls of the active rod can cause excitation of modes whose propagation direction makes a large angle to the resonator axis and which lead to dissipation of the excitation energy (parasitic modes) [118,119]. The modes of a dielectric resonator are considered theoretically in [120]. An effective method of suppressing parasitic modes is roughening the side surface of the rod or the use of an immersion sheath [3,121,122].

Besides diffraction losses that depend on the resonator shape, solid-state laser resonators involve losses due to inactive absorption and light scattering in the medium. Data on the absorption and scattering in some media are given in Table VII. Usually the losses in the resonator are determined by measuring the dependence of the threshold intensity P_{thr} and the generation intensity P_g on the resonator-mirror transmission (see expressions (7)—(17)[11,28,105]). Typical plots of P_{thr} and P_g against the mirror transmission are shown in Fig. 10[11]. We see that, in accord with the conclusions of the elementary theory, there is an optical mirror transmission, for which the generation power is a maximum.

The losses σ_{thr} and σ_g measured in a number of active media are listed in Table X (the subscripts thr and g correspond to losses determined from the threshold and from the generation power). For crystalline media, $\sigma_g/2l$ is usually close to the value of the small-angle scattering coefficient. In a laser using high grade neodymium glass, σ_g is close to the average diffraction loss brought about by the modes (see expression (38))[105]. It is shown in [28,105] that $\sigma_{thr} > \sigma_g$; for the case of neodymium glass this is apparently due to the uneven distribution of the pumping over the cross section of the rod and to excitation of generation at threshold in only a small fraction of the rod cross section. In the case a large threshold ratio, saturation of the inversion leads to equalization of the inversion over the cross section, and the Q of the resonator increases. One of the possible causes of the lower loss in multimode generation may also be the presence of strong coupling between modes (see Sec. II).

Table X

Active medium	Resonator length, cm	Rod length l, cm	Rod diameter, cm	$\frac{\sigma_{thr}}{2l}$, cm^{-1}	$\frac{\sigma_g}{2l}$, cm^{-1}	Literature
$CaF_2 : Sm^{2+}$	3	3	0.8	0.1	0.02—0.03	11, 28
Neodymium glass	28	8	0.5	0.025	0.0055	105
$CaWO_4 : Nd^{3+}$	5	5		0.026		123
Ruby	32	6	0.7	0.02	0.030	124

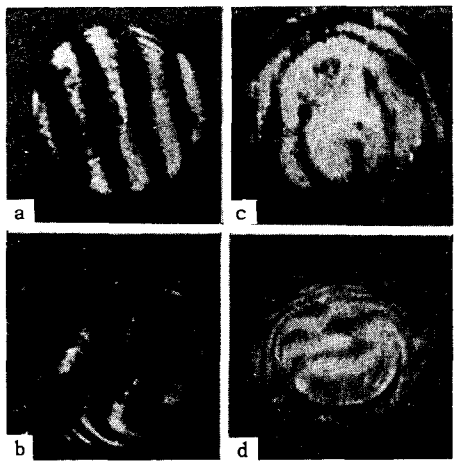

FIG. 11. Interference patterns of neodymium-glass (a, b) and ruby (c, d) before pumping (a, c) and after pumping (b, d).

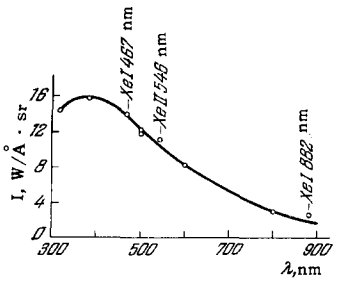

FIG. 12. Spectral distribution of radiation intensity of a flash lamp at the instant of maximum radiation. (d = 3 mm; l = 40 mm; C = 300 μF; U = 1 kV; L = 0).

In the case of optical pumping of the active rod, nonradiative transitions in the medium cause heating of the rod and deformation of the resonator [125-132]. If the heating is uniform, the rod becomes longer; consequently, and also as a result of the temperature shift of the luminescence line, the generation spectrum is displaced. The effect of uneven heating of the rod is stronger, since it causes distortion of the resonator shape, leading in turn to a change in all the laser emission characteristics, including the angular ones. In practice, the heating is always uneven, owing to the uneven distribution of the pumping over the rod cross section and the finite thermal conductivity of the material. The latter circumstance is particularly important for continuously or periodically operating lasers [129]. In the case of pumping by means of one short pulse, the temperature distribution in the rod coincides with the distribution of the heat release. The main factors causing deformation of the rod are the dependence of the refractive index of the medium on the temperature and the birefringence in the sample, caused by thermal stresses.* If we neglect the photoelastic effect, then the presence of a temperature drop ΔT in the rod gives rise to an optical path difference ΔL in the rod, equal to

$$\Delta L = l\frac{d\varkappa}{dt}\Delta T.$$

Examples of interference patterns characterizing the thermal deformation of the resonator are shown in Fig. 11.

To eliminate thermal deformation it is necessary to ensure uniform pumping of the active rod, which in practice is difficult to realize. More promising is the development of pumping systems that ensure axially-symmetrical distribution of the pumping, leading to spherical deformation of the resonator. In this case the resonator Q may increase (see, for example, [105]), and optical compensation of the deformation is also possible [105,127,130,180].

3. Optical Pumping Systems

The system for optically pumping a solid-state laser consists of a pumping source and a device for focusing the pump radiation on the active rod (illuminator). It affects not only the energetics of the laser but also, by shaping the pump-radiation field in the rod, the angular characteristics of the emission.

a) Pump sources. The main requirements that must be satisfied by a pump source is a large radiation energy yield in the absorption bands of the active medium and high intensity, making it possible to produce in the active rod a radiation density much in excess of threshold.

The sources most widely used at present are plasma sources—tubular xenon flash lamps and xenon and mercury arc lamps. The requirements spelled out above are to some degree contradictory in the case of plasma sources. To ensure a large radiation yield it is desirable that the source have a selective emission spectrum corresponding to the pump bands. At the same time, to obtain a large brightness, the

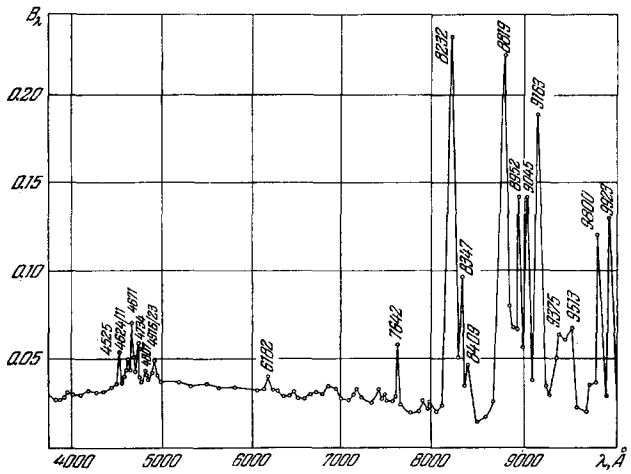

FIG. 13. Spectral distribution of brightness (W/cm² Å-sr) of the emission along the axis of a xenon arch-lamp discharge channel (d = 3 mm, p = 8 atm, P_e = 4.45 kW).

*When $l \gg D$, the bending of the end surfaces of the sample is quite small and can be disregarded [129].

Table XI

Spectral intervals, nm	Energy yield, %		
	Xenon flash lamp [134]	Xenon arc lamps [136]	
	IFP-400, W_{eff} = 150 J, U = 1000 V	D = 3 mm*, p = 5 atm, P = 2.46 kW	D = 5 mm, p = 5 atm, P = 3.1 kW
400—500	7.5	4.5	4.0
500—600	6.8	4.3	3.8
600—700	5.2	3.5	3.6
700—800	3.3	3.4	3.8
800—900	2	9.3	11.6
900—1000	—	7.6	9.7
400—900	24.8	25	26.8
400—1000		32.6	36.5

*D – diameter of luminescent body.

Table XII. Energy yield of xenon flash lamp in the ruby and neodymium-glass pump bands

Active medium	Absorption band, nm	Energy yield, %	
		IFP-400, W_{eff} = 150 J, U = 1000 V	IFP-15000, W_{eff} = = 12 kJ, U = 3000 V
Ruby	390—440	3.4 } ~ 10	~ 17
	520—590	6.7 }	
Neodymium-glass	500—550	4.8	
	570—600	2.8	
	730—760	1.3 } ~ 11	
	790—825	1.2	
	865—890	0.8	

temperature and the density of the electrons in the source plasma must be high, and then the plasma emission spectrum becomes continuous [133]. Figures 12 and 13 and Tables XI and XII show certain characteristics of xenon flash and arc lamps [134-136]. It is seen from the foregoing data that the emission spectrum of flash lamps is continuous and that of arc lamps is for the most part a line spectrum. The brightness temperature is (1—1.8) × 10^4 °K in the former case and (4—7) × 10^3 °K in the latter. The radiation energy yield of flash lapms depends little on the discharge conditions and the lamp parameters, increasing with increasing luminescent body in the lamp [134,135,137]. Under the normally employed operating conditions of flash lamps for pumping, the discharge plasma is practically opaque in the spectral region 530—900 nm during the pulse duration (measured at 0.3 of maximum) [137,50]. The discharge brightness in tubular xenon lamps is limited by the mechanical strength of the quartz tube. The limiting electric energy per flash, above which the flash lamp is damaged, can be estimated from the relation [134]

$$W_{lim} \simeq K\sqrt{t_{pul}},$$

where t_{pul} is the duration of the flash, and K is a constant that depends on the construction and dimensions of the lamp. The radiation intensity of flash lamps can be increased at the expense of shortening the flash duration by using the so-called double-pulse mode, in which a short powerful pulse (10—50 μsec) is superimposed on a relatively long discharge pulse (greater than 100 μsec) [138-140]. This method of operating the lamp provides a much higher value of W_{lim}, because the long pulse effects preliminary plasma formation. It must be borne in mind that the ultraviolet component of the lamp emission increases in such a mode.

Use of electrodeless argon flash lamps for pumping is now under study [141,142]. These lamps yield intense flashes of 1—10 μsec duration at repetition frequencies up to 100 Hz.

Besides xenon and mercury tubular arc lamps, continuously-acting lasers are optically pumped by iodine incandescent lamps (laser based on $CaF_2:Dy^{2+}$, YalG: Nd^{3+} [144,145]) and also by solar radiation (laser based on $CaF_2:Dy^{2+}$ [146,147], $CaWO_4:Nd^{3+}$ [147], YAlG: Nd^{3+} [148], and neodymium-glass [149]). Continuous lasing of ruby was attained with the aid of mercury arc lamps [150,151]. The energy yield of the radiation from such sources is listed in Table XIII.

The majority of the aforementioned pump sources have a continuous emission spectrum, so that their efficiency is relatively low. In this respect, interest attaches to pump sources which have not yet been fully developed technically, but which provide highly

Table XIII

Spectral intervals, nm	Energy yield, %			Radiation power density of the sun, W/cm²
	Iodine lamp, D = 5 mm [145]		Mercury arc D = 2 mm, p = 75 atm, P = 1 kW	
	P = 0.6 kW	P = 2.88 kW		
400—500	0.11	1.9	—	$2.01 \cdot 10^{-2}$
400—450	—	—	8	—
500—600	0.7	3.7	10	$2.02 \cdot 10^{-2}$
600—700	1.66	5.2	10.4	$1.6 \cdot 10^{-2}$
700—800	2.67	5.4	—	$1.32 \cdot 10^{-2}$
800—900	3.5	5.4	—	$1.06 \cdot 10^{-2}$
900—1000	4.25	5.4	—	$0.83 \cdot 10^{-2}$
400—1000	12.9	27.0	—	—
700—1400	—	—	7.6	—

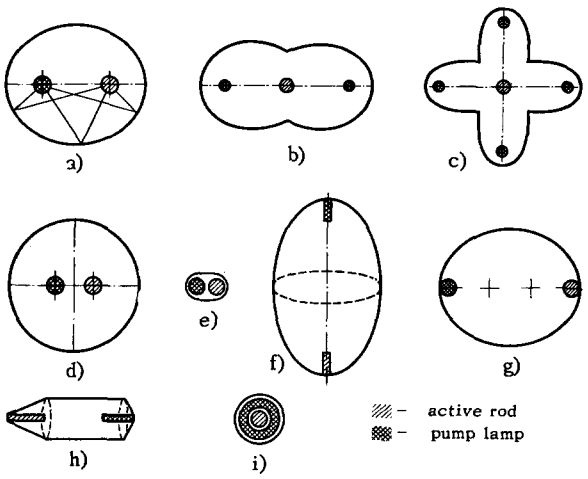

FIG. 14. Illuminators: a) elliptic cylinder [158]; b), c) many-ellipse cylinders [158,159]; d) circular cylinder [161]; e) close-packed illuminator [163,162]; e) ellipsoid of revolution [164,151]; g) elliptic cylinder with the rod and lamp placed outside the foci [164]; h) cylinder with cones [165]; i) coaxial system [166].

monochromatic radiation—semiconductor and cathode luminescence radiators. GaAs diodes, whose emission wavelength lies close to 0.84 μ, were used to excite generation in $CaF_2:U^{3+}$ crystals [152] and in $CaWO_4:Nd^{3+}$ crystals [153]. While having a high efficiency (up to 50% at T = 20°K), GaAs diodes have so far not yielded large radiation power, making their use as pump sources difficult.

A laser based on $CaWO_4:Nd^{3+}$ and pumped by a cathodoluminor is described in [154]. The theoretically possible maximum energy yield of cathodoluminors is 25—30% [155,156], and the value attained in practice is 20% (ZnS · CdS-Ag, $\lambda_{em_{31}} \simeq 580$ nm) [155]. The maximum emission power from a unit of luminor surface is limited by its thermal damage and by saturation effects, and does not exceed 10—30 W/cm^2 [154,155]; this, just as in the case of GaAs diodes, limits the application of cathodoluminors for optical pumping.

A pumping source providing intense radiation of short duration may be based on the pinch effect, but the energy yield of such a source is smaller than that of xenon lamps [157].

b) Illuminators. Many different illuminator configurations have been developed by now, the principal ones being shown in Fig. 14. With the exception of the case shown in Fig. 14i, all illuminators use the widely popular straight cylindrical lamps. The main characteristics of the illuminator are its efficiency ω, equal to the ratio of the radiant flux incident on the surface of the active rod to the total flux radiated by the lamp, and the uniformity coefficient γ, equal to the ratio of the pump density averaged over the rod cross section to the maximum density [50]. The value of ω, which greatly influences the energy parameters of the laser, is determined by the configuration and by the reflection coefficient of the illuminator surfaces, the transparency of the lamp and of the rod, and the ratio of their dimensions. The coefficient γ is determined both by the geometry of the illuminator and by the optical density of the rod. It must be noted that γ is no less an important parameter than ω: besides affecting the laser energetics (see expressions (7′) and (9′)), it greatly influences the character of the thermal deformation of the resonator and, accordingly, the angular and spectral characteristics of the laser emission. The values of the threshold pump energy and the generation intensity at small excesses over threshold greatly depends on the coefficient γ: if the pump is highly uneven ($\gamma \ll 1$), relatively low thresholds can be obtained even in an illuminator of low efficiency [50]. At large threshold ratios, the generation intensity is determined principally by the efficiency ω of the illuminator. Illuminators in the form of elliptic and circular cylinders and closely packed illuminators (Figs. 14a, d, e) are most widely used, being simplest and of adequate efficiency. A shortcoming of a closely-packed illuminator is the highly uneven distribution of the pumping. Interest attaches, especially from the point of view of uniform pumping, to illuminators in the form of ellipsoids of revolution and of cylinders with cones (Figs. 14f, h). However, owing to certain operating inconveniences, these illuminators have not been widely used. A pump system with a coaxial lamp and a cylindrically placed active rod (Fig. 14i) ensures axially-symmetrical distribution of the pumping; its shortcoming is the difficulty of obtaining high pump radiation density in the rod, especially if the latter is small. It should be noted that such a pump system (with a large rod) was used in [166] to obtain a neodymium-glass laser having an

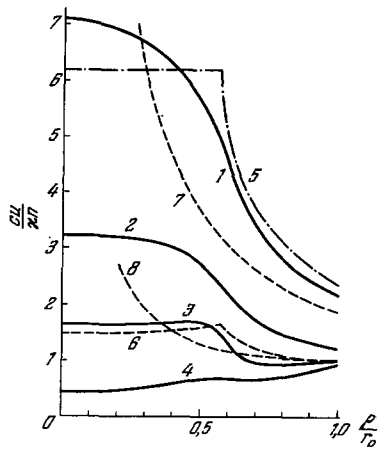

FIG. 15. Pump density distribution (u) over the cross section of a polished ruby rod: k — pump-radiation absorption coefficient, cm^{-1}; r_0 — radius of rod, ρ — running radius. 1,5,7 — $kr_0 = 0$, 2 — $kr_0 = 0.625$, 3,6,8 — $kr_0 = 1.25$, 4 — $kr_0 = 2.5$; 1,2,3,4 — radiation isotropically incident on the surface of the rod, 5,7 — radiation isotropic in a plane perpendicular to the cylinder axis, 6,8 — radiation incident perpendicular to the cylinder surface.

Table XIV

Type of illuminator	Major axis, mm	Diameter, mm	Distance between axes of the lamp and rod, mm	Dimension of lamp and rod: Diameter, mm	Dimension of lamp and rod: Lamp	ω, experimental	ω, calculated
Elliptic cylinder	100		40	5	45	0.36	0.38
	100		40	8	80		0.49
Circular cylinder		19	9	8	80		0.61
		20	9	8	80	0.58	0.64
		30	9	8	80	0.75	0.67
		44	9	8	80	0.67	0.62
		60	9	8	80	—	0.6
		70	9	8	80	0.66	—
		77	9	8	80	0.64	0.56

efficiency of 5.1% (for more details see Sec. IV, 1). Silver or aluminum coatings with selective reflection are deposited on the surfaces of the illuminators [167].

The efficiency of illuminators in the form of elliptic or circular cylinders, with optimal parameters, can reach 0.7—0.75 [50].

To obtain larger pump densities, multilamp illuminators with elliptic reflectors are used (Fig. 14b, c). In such illuminators, the diameter of the lamps is usually smaller by a factor 1.5—2 than the diameter of the rod. When the lamp and rod diameters are equal, the increase in the pump density (compared with single-lamp illuminators) does not exceed a factor 1.3—1.7, while the efficiency of the illuminator is decreased [159].

Calculations for illuminators—elliptic (including multi-lamp) and circular cylinders—is described in [159,160,50]. Table XIV lists the results of a comparison of the calculated values of ω and those obtained experimentally for a number of illuminators, for equal lamp and rod dimensions [50]. Illuminating systems using helical lamps are less efficient than those considered above, but they are sometimes used for pumping rods of large cross sections [122]. The distribution of the pump density over the rod cross section was investigated experimentally in [50,168]

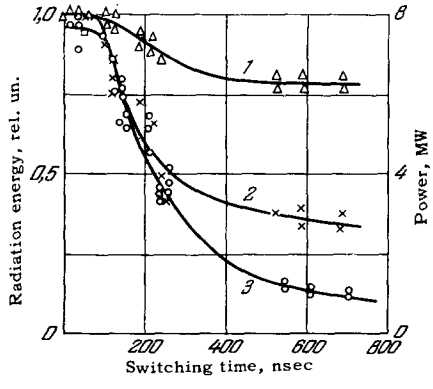

FIG. 16. Dependence of the total laser emission energy (1), the energy of the first pulse (2), and the power of the first pulse (3) on the shutter switching rate.

(neodymium glass) and [169] (ruby), and calculations of the distribution were performed in [169-171]. Figure 15 shows the pump distribution over the rod cross section, calculated without allowance for the bleaching of the material [170] (allowance for bleaching is made in [171]. The experimentally measured value of the uniformity coefficient for illuminators in the form of elliptical or circular cylinders is 0.7—0.75 [50].

In conclusion we note that to increase the pump radiation density in rods the latter are frequently surrounded by an immersion sheath (see, for example, [158]). If the sheath is sufficiently thick, the gain reaches a value equal to κ.

4. Optical Shutters

The main requirement imposed on the shutter of a monopulse laser is rapid switching and slow losses in the open state. It is known that in the case of instantaneous switching of the shutter, the generation pulse lags the instant of switching by a delay $t_{sh} \sim \Delta t/k_0 l$, where Δt is the time of flight of the quantum in the resonator and $k_0 l$ is the initial amplification in the rod [10,25,36]. In practice $t_{sh} \simeq 20$—80 nsec. It is obvious that the time t_f necessary for complete opening of the shutter, should be shorter than t_{sh}, and therefore it can be assumed that the shutter provides practically instantaneous switching if $t_f \leq 20$ nsec. Slow switching of the shutter ($t_{sh} \geq 20$ nsec) usually leads to excitation of several generation pulses in succession, i.e., to violation of the monopulse regime (see, for example, [172]).

Figure 16 shows the effect of the value of t_f on the energy characteristics of a ruby laser with a Kerr cell [173]. Violation of the monopulse regime occurs when $t_f > 100$ nsec, and is accompanied by a decrease in the energy and power of the first pulse (curves 2 and 3).

Let us examine briefly the most widely used shutter types.

The existing shutters can be divided into three classes: optical-mechanical, electrooptical, and passive saturable.

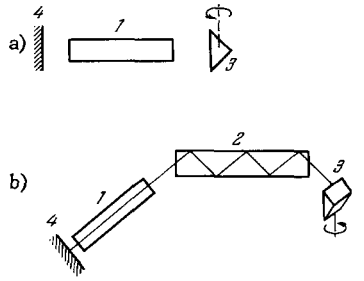

FIG. 17. a) Diagram of laser with rotating prism, b) Diagram of laser with Daly-Sims shutter. 1 – active rod, 2 – plane-parallel plate, 3 – rotating prism, 4 – semitransparent mirror.

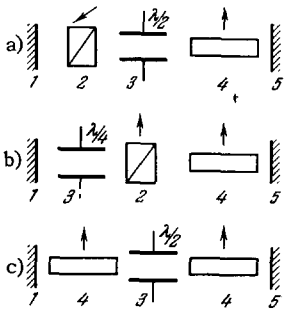

FIG. 18. Diagrams of lasers with electro-optical shutters. 1,5 – 100% and semitransparent mirrors, respectively; 2 – polarizer; 3 – shutter cell; 4 – active rod. The relative orientations of the polarization planes are designated by the arrows.

A rotating total-internal reflection prism, acting as a resonator mirror, is the simplest shutter suitable for work with all principal active media (Fig. 17a). The rotary prism speed necessary to ensure the monopulse regime depends on the length of the resonator and on the initial gain in the medium. For a ruby laser ($L \approx 50$ cm) the required speed is usually not less than 5×10^4 rpm [172], and for a neodymium-glass laser not less than 2×10^4 rpm [174].

A substantial reduction in the switching time is ensured by using a plane-parallel total-internal-reflection plate in conjunction with the rotating prism (Fig. 17b) [175]. Thus, at a prism speed of 3×10^4 rpm we have $t_f \simeq 1000$ nsec (for a ruby laser), and ~70 nsec in the case when a plate with 12 reflections is used. An advantage of such a shutter is that the off time is much longer than the on time.

Shutters based on the Kerr and Pockels effects have the lowest inertia and afford a switching time $t_f \leq 20$ nsec. In the Kerr cell, one uses liquids having birefringence and a large Kerr constant, such as nitrobenzene [179], and in the Pockels cell one uses birefringent ferroelectric crystals, such as KH_2PO_4 (KDP), KD_2PO_4, and others [176,177]. Diagrams of ruby lasers with shutters made of Kerr or Pockels cells are shown in Fig. 18 [27,35]. In Fig. 18b, a constant blocking voltage is applied to the plates of the shutter to ensure a path difference of $\lambda/4$, causing the shutter to be closed. When this voltage is removed by application of a pulse, the shutter opens. In Fig. 18a, the shutter is opened by applying to its plates a voltage pulse producing a path difference $\lambda/2$. The polarizer is used in these schemes for a more reliable shutting of the shutter, making it possible to produce a large inversion in the rod. Figure 18b shows the diagram of a monopulse generator with two crystals and a shutter between them [178].

To increase the power of the monopulse generator, a scheme was proposed in [35] for rapidly varying the transmission coefficient of one of the resonator mirrors from ~0 to ~100% at the instant when the maximum radiation density is attained in the resonator. The generation pulse duration approaches in this case $2\Delta t$. A modification of such a scheme was realized in a ruby laser [281], and also in a laser using glass with Nd^{3+} and $CaWO_4:Nd^{3+}$ [282]. Kerr and Pockels cells can be used in monopulse generators with neodymium glass [174], an additional polarizer being required to polarize the radiation of the glass.

Table XV lists the values of the voltages required to produce a path difference $\lambda/2$ in different substances at wavelengths 0.695 and 1.06 μ.

Recently much attention has been paid to passive shutters, based on the effect of bleaching certain

Table XV

Substance	Voltage necessary to produce a path difference of $\lambda/2$, kV [176,179]		Type of cell
	$\lambda = 0.695$ μ	$\lambda = 1.06$ μ	
KH_2PO_4(KDP)	~ 10	15.5	Pockels
KD_2PO_4	4.3	6.6	
$NH_4H_2PO_4$(ADP)	~ 12	~ 20	
KH_2AsO_4	7.9	12	
RbH_2PO_4	9.3	14.2	
Nitrobenzene	$U = \frac{0,3d}{(2lB_\lambda)^{1/2}}$ kV d — linear aperture l — length of shutter plates $B_{\lambda=0.695} \simeq 2.5 \cdot 10^{-5}$ cgs esu. $B_{\lambda=1.06} \simeq 1.5 \cdot 10^{-5}$ cgs esu. For $d = 1$ cm, $l = 8$ cm:		Kerr
	~ 15	~ 20	

Table XVI

Active medium	Dimensions of active medium		Resonator			Working temperature, °K	Pump source	Operating regime	Threshold, J	Radiated energy and power	Efficiency, %	Literature
	D, cm	l, cm	L, cm	R, %	Configuration							
Ruby	0.8	8	30	50	Planar	300	Xenon lamp	Pulsed, uncontrolled	150	4 J	0.7	163
Ruby	0.64	7.6	30	50	Planar	300	Xenon lamp	Monopulse–rotating-prism shutter	80	0.07 J 2 MW	0.035	273
Ruby	1.6	3×24+ +12	200	5	Planar	300	Xenon lamp	Monopulse, shutter–Kerr cell and passive filters	—	15 J 8 GW	—	196
Ruby	1.55 1.9	20+20	100	5	Planar	300	Xenon lamp	Monopulse, passive shutter		20 J 1 GW	0.095	285
Ruby	0.2	2.5	2.5	90	Spherical	300	Mercury capillary lamp	Pulsed, uncontrolled with frequency 100 Hz	3	2 W	0.22	280
Glass: Nd^{3+}	1.8	94.1	100	3	Planar	300	Coaxial xenon lamp	Pulsed, uncontrolled	5000	700 J	5.1	166
Glass: Nd^{3+}	0.8	80	28		Spherical	300	Xenon lamp	Pulsed, uncontrolled monopulse, shutter–rotating prism	9	1.2 J 2 J	2 0.8	105
Glass: Nd^{3+}	4.5	3×25	100	4	Planar	300	Xenon lamp	Monopulse, passive shutter		120 J 6 GW		286
Glass: Nd^{3+}	1.8	30.5	500		Planar	300	Xenon lamp	Monopulse, passive shutter (self-capture modes), Kerr shutter (extraction of energy in accordance with [35])		0.2 J 25 MW		287
YAlG : Nd^{3+}	0.3	3	50	99.4	Spherical $r = 25$ cm	300	Iodine lamp	Monopulse with frequency 100 Hz, shutter-rotating prism	500 W	1.5 W	0.015	144
YAlG : Nd^{3+}	0.3	3	3		Spherical $r = 5$ cm	300	Sun, mirror diameter 61 cm	Continuous		1 W		148
YAlG : Nd^{3+}						300	Argon arc	Continuous		42 W	0.085	197
CaF_2 : Dy^{2+}	0.7	7				77	Xenon arc lamps	Monopulse with frequency 200 Hz, shutter–rotating prism		0.05 W		65

liquids in glasses under the influence of laser radiation. In ruby lasers one uses for this purpose solutions of cryptocyanine [180,181], phthalocyanines of metals [181-183], glasses containing selenides and sulfides of cadmium [167,184,185]. In neodymium lasers one uses solutions of polymethine dyes [186-188]. The bleaching of the crypto- and phthalocyanines is the result of the depletion of the ground state when the laser radiation is absorbed.

The energetics of the processes occurring in a laser with a shutter of this type is considered in [189,181,190]; it is assumed here that the absorption line is homogeneously broadened in the material of the shutter; this is confirmed by the results of [192,193]. The energy generated by a laser with a three-level active medium and a passive shutter can be determined from the relation

$$W = \frac{E \ln 1/R}{4lk_{thr}} \left\{1 - \frac{k_I}{k_0} - \frac{\Lambda}{\Lambda_{sh}}\left(1 - \frac{k_{II}}{k_0}\right)\left[1 - \left(\frac{k_I}{k_0}\right)^{\frac{\Lambda}{\Lambda_{sh}}}\right]\right\}, \quad (29')$$

where Λ and Λ_{sh} are the cross sections for stimulated emission in the active medium and for absorption in the bleached medium; the remaining symbols are the same as in (29). From a comparison of (29') and (29) we see that for a passive shutter to operate effectively it is necessary to have $\Lambda_{sh}/\Lambda \gg 1$. In the media employed, $\Lambda_{sh}/\Lambda = 10^4$—$10^5$. Glasses containing selenides and sulfides of cadmium are bleached by absorption of laser emission as a result of a shift of the absorption-band edge [193].

Besides the most commonly used shutters mentioned above, the literature includes descriptions of laser Q-switching with ultrasonic pulsed light modulators [194], by application of a magnetic field [195,283] or an ultrasonic field [34] on the active medium, and by introducing into the resonator thin films that are destroyed by the action of the radiation [106].

Passive shutters are also used in monopulse generators to realize a mode self-capture regime (see Sec. IV, 4). Another interesting application of passive shutters that become bleached only at a finite value of the light-wave field and having large active-particle concentration [284], is their use as decoupling elements, which make it possible to reduce greatly the duration of the generation pulse in multistage lasers [196].

IV. CHARACTERISTICS OF LASER EMISSION

1. Energy Characteristics

The main energy characteristics of a laser are the threshold pump intensity, the generation emission intensity, and the efficiency. Table XVI lists the energy parameters of a number of lasers. The maximum efficiency (50%) has been attained at present in neodymium-glass lasers. The highest generation pulse repetition frequencies (100—300 Hz) have been obtained in a monopulse laser using continuous pump sources [65,144,151]. We confine ourselves in this sec-

Table XVII

Active medium	Pump source	Limiting efficiency, %
Neodymium glass	Pulsed xenon lamp IFP-15000	~ 6
Ruby	The same	~ 2 *)
$CaWO_4 : Nd^{3+}$	Xenon arc lamp	~ 1.7
$CaF_2 : Dy^{2+}$	Iodine incandescent lamp	~ 1.3

*Account is taken of absorption from the upper working level.

tion to problems connected principally with the limiting parameters of solid-state lasers and their limitations.

Efficiency. The maximum efficiency of a laser, for a specified pump source, can be obtained under the following conditions:

1) the pump system efficiency $\omega = 1$;

2) losses in resonator much smaller than ln 1/R;

3) pump intensity much higher than threshold, i.e., $n \gg 1$;

4) optical density of active rod in the pumping bands much larger than unity.

When these conditions are satisfied, we can obtain from (9) or (17) and (9′) an expression for the limiting efficiency:

$$\frac{W_g}{W_{eff}} = \sum_i \frac{\nu_g}{\nu_{pi}} \eta_{1i} F_i.$$

Table XVII lists tentative values of the limiting efficiency, calculated by using the data of Sec. III, for a number of active media. As seen from Tables XVI and XVII, the efficiencies attained by now in neodymium-glass and ruby lasers are close to the limiting values. The efficiency of these lasers can be increased further only by increasing the optical yield of the pump sources and by using sensitization of the luminescence of the active media. The efficiency of a laser operating in the monopulse regime is as a rule much lower than the efficiency of a laser operating in the pulsed regime. This is caused by two factors:

1) deterioration of the resonator Q by introduction of the shutter;

2) influence of superluminescence and bleaching of the medium (an appreciable decrease of τ as a result of superluminescence was observed experimentally for ruby in [30], for $CaF_2 : Dy^{2+}$ in [29], and for $CaF_2 : Sm^{2+}$ in [28]. An important factor in ruby is also the increase of absorption from the ^2E level at large inversions.

Generation Intensity. Let us consider the main factors limiting the possibility of attaining large generation intensities.

1) In the monopulse regime, the generation intensity is limited by superluminescence and by bleaching of the medium (see Fig. 3).

2) Thermal effects. The heating of the active material, which is inevitable in the case of optical pumping, imposes limitations on the pump energy that can be supplied. Owing to the deterioration of the luminescence properties of the medium (line width, quantum yield), heating raises the threshold and decreases the generation radiation yield (see, for example [198]). We have already pointed out that the resonator Q is adversely affected by thermal deformation of the rod if the latter is unevenly heated. Deformation and the associated thermal stresses [129] can cause damage of the rod. Interest attaches in this connection to materials having a high strength, high thermal conductivity, and low thermal coefficient of expansion (ruby, garnet).

3) Damage of the active rod under the influence of the generation radiation. It is known that when the generation radiation density is appreciable, the active material becomes damaged [199-201]. Neodymium glass is characterized by the appearance of cracks inside the rod [201], and ruby by prickles on the end surfaces of the rod [199]. The damage mechanism and the associated nature of the interaction between the radiation and the medium have not been sufficiently investigated. Apparently an appreciable role in the appearance of cracks in neodymium glass is played by microscopic platinum inclusions, which absorb radiation and cause local heating of the glass [200,201]. When the platinum inclusions are eliminated, the limiting load in neodymium glass increases from 10^8 W/cm^2 to 10^9 W/cm^2 and more (pulse duration 100 nsec). In ruby, the limiting load amounts to $\sim 3 \times 10^8$ W/cm^2 [200], and for crystals with 60° orientation of the optical axis, the limiting load is 20—30% higher than for 90° orientation. In [199], the hypothesis has been advanced that the destruction of the ruby is due to the occurrence of an elastic wave in stimulated Mandel'shtam-Brillouin scattering. However, it is shown in [288] that the cause of the damage to the ends of the rod is spark breakdown at the surface, produced under the influence of the laser emission field.

A definite role in the damage to the media is apparently played by self-focusing of the radiation, due to nonlinear variations of the refractive index under the influence of the strong light fields. These phenomena can come into play even at radiation powers $\sim 10^6$—10^7 W [274].

4) One of the factors that can lead to a limitation of the intensity of the stationary generation is the finite time of nonradiative relaxations in the active medium. An experimental study of the dependence of the generation intensity on the pump power shows that for all the basic active media this dependence retains its linear character up to very high pump levels (see,

for example,[67,11]). The threshold ratios at which the generation power becomes saturated can be determined with the aid of (12). For neodymium glass, in accordance with the data of [26,191] ($d_{43} \approx 1.6 \times 10^4$ sec^{-1}; $d_{21} \approx 10^8$ sec^{-1}), saturation should be observed at $n \gg 350$. Thus, this limitation is not significant for the existing pump sources.

5) Nonlinear effects in a medium at large radiation densities, which can lead to a limitation of the laser power, are considered in [202]. The estimate given there shows that multiphoton processes limit the ruby-laser power to $\sim 10^{12}$ W/cm^2.

2. Spectral Characteristics

In considering the laser emission spectra one can speak of their gross structure—location of the emission bands—and the fine structure of these bands.

The position of the emission bands (the generation wavelength) is closely related to the spectral characteristics of the active medium—the structure of the luminescence centers, the level scheme, etc. When varying the resonator Q and the active-medium temperature, jumplike changes in the generation wavelength are frequently observed, this being the result of the competition between the different transitions at which generation is possible. Thus, in laser based on $CaF_2:U^{3+}$ crystals with tetragonal-symmetry centers, the generation takes place in accordance with a three-level scheme ($\lambda = 2.22\ \mu$) when the resonator Q is low; at high Q, generation is in accordance with a four-level scheme, with $\lambda = 2.51\ \mu$ when $T > 250°K$ and $\lambda = 2.43\ \mu$ when $T < 250°K$ [11,81]. Similar changes in the generation wavelengths were observed also in the crystals $CaF_2:Sm^{2+}$ [11], $CaWO_4:Nd^{3+}$ [203], $CaF_2:Nd^{3+}$ [204]; in ruby, the generation band splits into two components, at $T \simeq 78°K$ [205].

Particularly complicated are the generation spectra that can be observed when the medium contains interacting centers of different structure. Examples are the spectra of lasers with $CaF_2:U^{3+}$ crystals, which contain centers of different symmetry [81]. Owing to the resonant excitation-energy transfer and the deactivation of the centers of one type as a result of induced transitions caused by emission from centers of another type, a jumplike change of λ was observed within the course of a single generation pulse, as well as simultaneous generation at two or even three wavelengths. The foregoing phenomena can be easily interpreted within the framework of the method of kinetic equations, with due allowance for the concrete features of the level scheme of the medium (see, for example, [11,81]).

The fine structure of the generation emission bands is determined principally by the properties of the resonator, and also by the width and character of the luminescence line broadening. The excited modes are investigated experimentally with the aid of high-resolution spectral instruments [52,67,95,206-209], by observing beats at difference frequencies [114,210,211], and also by investigating the spatial structure of the radiation [108,114,206].

The observed frequency difference between neighboring modes with different axial indices is usually close to $C/2\kappa L$ for resonators with flat mirrors; for angular modes this difference is 3×10^{-4}—7×10^{-3} cm^{-1}, which is much higher than the calculated values (see Sec. III, 2). However, allowance for the deviations of the resonator shape from ideal results in satisfactory agreement between the calculated and experimental data [211,212].

Time scanning of the spectrum reveals that in the case of the spiked generation regime, each spike contains either one mode (small threshold ratio, narrow luminescence line) or a set of modes with different axial indices; this set changes from spike to spike [95,206,208,210,213]; when the pump power is increased, the number of modes per spike is usually increased. Similar regularities were observed also for the angular modes [206,214,215]. We note that in the quasistationary (spikeless) regime, there is likewise a continuous succession of excited modes, which can be either regular or random [52,212].

The total spectral width of the generation band is determined by the number of the excited modes with different axial indices. For a homogeneously broadened luminescence line, the width of the generation spectrum is quite small. Thus, for ruby this width is usually 0.1—0.5 Å for $T = 300°K$ [208,213]. The time-averaged spectral distribution of the radiation has usually a bell shape [52]. The width of the distribution increases with increasing pump power (at small threshold ratios [95,209]) and with increasing luminescence line width, which in turn can be due both to an increase in temperature and to an increase in the activator concentration (e.g. [216]).

All these regularities can be interpreted within the framework of the Tang-Statz model, in which account is taken of the spatial mode competition (Sec. II. 2). A quantitative comparison of the experimental and the calculated data was carried out for the case of a $CaF_2:Sm^{2+}$ laser [52] operating in the quasistationary regime; the agreement between these data is perfectly satisfactory (Fig. 19).

To eliminate nonuniformity in the distribution of the radiation in individual modes along the resonator axis, which leads to multimode generation, a traveling-wave ring laser was used in [93], a laser with axial displacement of the active rod during the time of generation in [217], and in [218] a laser was used in which the components of different polarization, corresponding to one mode, were shifted relative to one another along the resonator axis by $\lambda/4$, so that the total radiation intensity was uniformly distributed along the axis. In all these cases, the expected sharp

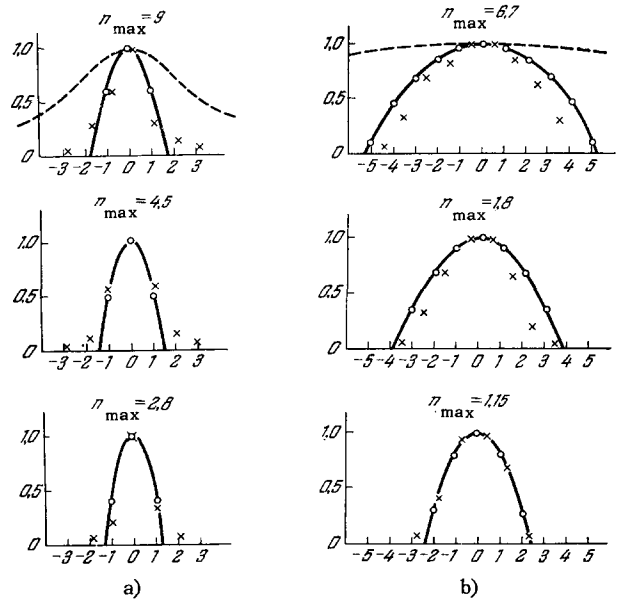

FIG. 19. Distribution of generation intensity among the spectral bands as a function of $\Delta\nu/(c/2\kappa L)$. Sample temperature: a – 15°K, b – 40°K, × – experimental data (time-integrated radiation intensity pertaining to individual bands, in relative units), O – calculated data, dashed – luminescence line contour.

reduction in the generation-spectrum width was observed.

For an inhomogeneously broadened luminescence line, the width of the generation spectrum can be quite large. In particular, the width of the generation spectrum of a neodymium-glass laser exceeds by several times the value calculated with the aid of (36) and reaches ~50 Å (for example,[208,219]).

The spectral width $\Delta\nu_m$ of individual modes is quite small and is determined by the duration of the spikes Δt ($\Delta\nu_m\Delta t \approx 1$)[207,210,220,95]. A value of $\Delta\nu_m\Delta t < 1$ for a ruby laser was obtained only in[221], thus evidencing the presence of coherence between individual spikes.

The presence of negative anomalous dispersion in the active medium leads to the effect of mode "pulling" in the laser, i.e., to a decrease in the frequencies between the modes with different axial indices. This effect was observed in lasers based on ruby[210], $CaF_2:Dy^{2+}$, and $CaF_2:U^{3+}$[95]. For a Lorentz line shape, the magnitude of the pulling, determined by the ratio of the frequency difference between neighboring axial modes $\Delta\nu$ to the quantity $\Delta\nu_a = C/2\kappa L$, is given by the relation[95]

$$\frac{\Delta\nu}{\Delta\nu_a} = \frac{\Delta\nu_л}{\Delta_{lum}+\Delta\nu_r},$$

where $\Delta\nu_r = C\sigma/4\pi\kappa L$ is the width of the resonator pass band. Thus, the pulling effect is the larger the smaller $\Delta\nu_l$ and the lower the Q of the resonator. For a Gaussian line shape, besides the "condensation" of the spectrum, the condition for equal spacing of the axial modes is violated. In accordance with the foregoing, in ruby the pulling effect turns out to be small, whereas in $CaF_2:Dy^{2+}$ (T = 80°K) the value of $\Delta\nu/\Delta\nu_a$ was 0.7—0.9 and the axial modes were no longer equidistant.

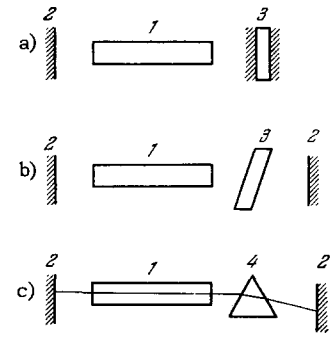

FIG. 20. 1 – active sample; 2 – mirror; 3 – Fabry-Perot interferometer; 4 – dispersing prism.

The generation spectrum is strongly influenced by thermal effects. The heating of the sample by the optical pumping leads to a shift of both the luminescence line and of the resonant mode frequencies, owing to the change in the optical length of the rod. A drift of the generation band, due to the shift of the luminescence line, was observed in ruby lasers[205,222]. The shift of the mode frequency, due to the change in the optical length of the resonator, is described in[223]; in the case of a prolonged generation pulse, a smooth shift of the mode frequency, corresponding to the change in the resonator length, was accompanied by jumplike frequency shifts, due to the faster temperature shifts of the luminescence line. Similar thermal effects were observed in laser based on $CaF_2:Sm^{2+}$[209,52] and $CaF_2:Dy^{2+}$[95]. For a ruby laser, the shift in the generation spectrum for a change in temperature from 30 to 350°K is 12—15 Å[222], and for a $CaF_2:Dy^{2+}$ (at T = 20°K—80°K) it is 2 Å.

The laser generation band width is narrowed by means of spectral selectors. The main types of resonators with spectral selectors are shown in Fig. 20. The most frequently used selector is a Fabry-Perot interferometer, used either as one of the resonator mirrors (Fig. 20a), or placed in the resonator in such a way that its axis is inclined at a small angle to the resonator axis (Fig. 20b). Since the reflection coefficient of the interferometer has, in the case of small angles of incidence, a periodic dependence on the radiation frequency, with period ~C/2t (t—optical thickness of the interferometer), the dependence of the resonator Q on the frequency turns out to be modulated at the frequency corresponding to this period. As a result, for different interferometer parameters one can observe both narrowing of the generation band (the modulation period is comparable with the generation line width), as well as a spreading

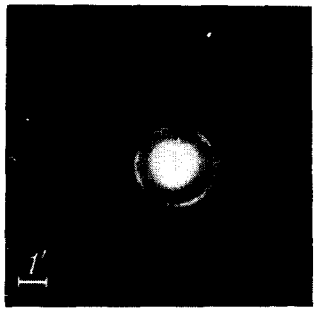

FIG. 21. Angular divergence of emission ($CaF_2:Sm^{2+}$ [16]).

out of the laser frequency spectrum*). To increase the selection effect, several standards are used simultaneously [226].

The use of two interferometer-selectors in a $CaWO_4:Nd^{3+}$ laser [227] has made it possible to reduce the number of axial modes from 400 to 1; in a neodymium-glass laser, the spectral width was reduced to 1 Å without changing the generation power [219].

Of interest is the so-called dispersion resonator (Fig. 20c), which makes possible selection and control of the generator wavelength as a result of the dispersion of the material of a prism placed in the resonator [229]. Such a resonator was used to obtain generation at the R_2 line of ruby [229]†, and to demonstrate the feasibility of controlling the wavelength of neodymium-glass laser within a wide range [232].

It must be noted that the spectral selection is usually associated with a certain decrease in the generation power, due both to the inevitable additional losses introduced into the resonator and to the decrease in the number of the excited centers participating in the generation when the generation spectrum is broadened or made narrower [233].

In conclusion, let us consider briefly the main experimental results on the spectra of monopulse lasers. The spectral characteristics of the emission of such lasers depend on the type of shutter employed. In a laser with an optical-mechanical or electrooptical shutter, the emission spectra have a complicated structure and are similar to the time-averaged spectra of lasers operating in the pulsed regime, but the width of the spectrum is somewhat smaller [40,97]. The use of spectral selectors (in view of the large gain in the medium in the monopulse regime, the selectors consist of plates or stacks without reflecting coatings) makes it possible to greatly reduce the generation spectrum: In [40], replacement of the reflecting mirror by a plate caused the spectrum of a ruby laser to narrow down from 0.3—0.7 Å to 0.05 Å; the use of a stack in a neodymium-glass laser has made it possible to narrow the spectrum down to 0.03 Å [97]. The use of passive shutters leads to an appreciable narrowing of the generation spectrum. For ruby in a resonator without a selector, a spectral width smaller than 0.02 Å was attained [180], and in a resonator with a selector, the value is less than 10^{-3} Å [234]. A spectral width smaller than 0.02 Å was observed in a neodymium-glass laser [235].

A possible explanation of the narrowing of the spectrum of a laser with passive shutter is that when this type of shutter is used the generation pulse builds up during its initial stage relatively slowly, at approximately the same rate as the individual emission spike in a laser without a shutter, so that the number of modes is approximately the same in both cases [234].

We note that in [236,237] the relatively narrow spectrum of the individual generation spike is attributed to the possible damping of modes with small Q during the prolonged transient time. Although such a point of view is at first glance plausible (see, for example, [27] concerning the influence of the rate of switching the shutter on the generation spectrum width), many details of the mechanism of spike formation are not clear and this question calls for further study.

3. Angular Divergence of the Laser Radiation

The far-zone radiation distribution of solid-state lasers with flat resonator mirrors is usually in the form of a spot surrounded by concentric rings (Fig. 21). The greater part of the total radiation intensity lies in the spot (see, for example, [16]), so that it is precisely the dimension of this spot which is defined as the angular divergence. As a rule this quantity greatly exceeds the diffraction limit, which is equal to $\alpha_d \simeq \lambda/D$. The reason for this difference may be either the excitation of a large number of angular modes or a large angular width of the radiation of individual modes.

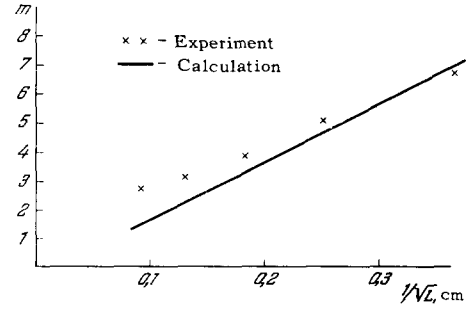

FIG. 22. Number of angular modes m as a function of the resonator length (neodymium glass [16]).

*The spreading of the spectrum was observed also in composite generators, consisting of several rods with partially reflecting end surfaces (see, for example, [224,225]).

†Generation at the R_2 line was also obtained by using a resonator mirror with a narrow-band reflecting coating [230] and by using the differences in the rotation of the polarization planes of the R_1 and R_2 lines in a quartz plate [231].

Inasmuch as the majority of the experimental data on the angular divergence are highly varied and insufficiently systematized, it is difficult to draw the line between the influences of these factors. In perfect resonators, as shown in Sec. III, 2, the angular divergence of the radiation of individual modes increases. Experimental investigations have shown, in accord with the theory, that even small distortions in the resonator shape are sufficient for an appreciable deformation of the modes. Thus, in the case of a ruby laser, the modes that could be identified with the modes of a planar resonator were observed only for isolated samples of crystals that were highly homogeneous optically ($\Delta L \simeq \lambda/10$); for rubies of medium quality ($\Delta L \gtrsim \lambda/4$) the modes were too distorted to be identifiable [238]. Considerable mode broadening was observed when the mirrors of a neodymium-glass resonator were only slightly misaligned: The mode angular divergence doubled when the angle between mirrors was 40″ (rod diameter 8 mm, resonator length 100 cm)[239]. A similar effect is exerted on the angular divergence by elastic or thermal deformation of the rod (see, for example, [214,128]).

If the active rod contains inhomogeneities with an axially-symmetrical refractive-index gradient, the angular divergence of individual modes can be interpreted quite adequately by using the deductions of the theory of spherical resonators (see Sec. III, 2)[240,108]. It must be noted that observation of individual angular modes is possible as a rule only at slight threshold ratios (angular selection will be discussed later)[108]. In the case of greater practical interest, that of large threshold ratios, a large number of modes is usually excited and the central spot in the far zone has no ordered structure [16].

The angle obtained in [241] for high-grade rubies was $\alpha \simeq \alpha_d$; α increased by a factor of several times with increasing pump energy; this increase was accompanied by low-frequency beats, pointing to the presence of several angular modes in the generation.

In the case of a planar resonator, it follows from (36) that the number of excited angular modes m is determined by the ratio of the nonselective and diffraction losses, and should therefore depend on the length L and the diameter of the resonator (see Table VIII and (39)). The dependence of the angular divergence α, and correspondingly of $m \simeq \alpha/\alpha_d$, of emission from a laser using high-grade neodymium glass on the resonator length was investigated in [16] (Fig. 22). Since the losses were close in this case to the diffraction value [105], it is possible to compare the experimental results with those of a calculation of the number of excited modes within the framework of the Tang-Statz model (relations (37) and (32)). As seen from Fig. 22, the agreement between the calculated and experimental data is perfectly satisfactory.

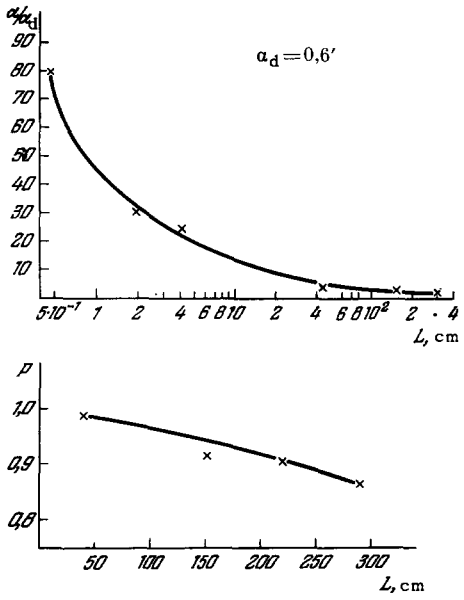

FIG. 23.

It was established here that the generation power remains practically unchanged when L increases, up to values corresponding to $\alpha = (1.5—2)\alpha_d$; at larger L, the decrease in the power becomes noticeable, which again corresponds to results of estimates within the framework of the Tang-Statz model [16]. It has turned out, in accord with (37), that α does not depend on the threshold ratio n if $n \gtrsim 2$. The data obtained in [16] allow us to conclude that the Tang-Statz model describes satisfactorily not only the time-averaged spectral characteristics of the laser emission (see Sec. IV, 2), but also the angular characteristics, provided the active medium and the resonators are of high grade. At the customarily employed resonator dimensions, one can regard as high grade those rods and resonators with a maximal optical-path difference $\Delta L \lesssim (0.05—0.1)\lambda$ (see Sec. III, 2). The angular divergence α in a laser with rod made of an inhomogeneous material, such as ruby, is relatively large. With increasing resonator length, α decreases but then the generation power begins to decrease rapidly long before α approaches the value α_d: the threshold pump power also increases [242]. Therefore, with increasing L the brightness of the laser beam reaches a maximum value and begins to decrease. This case can be qualitatively interpreted by assuming that in a less-perfect resonator even the lowest modes have a complicated structure [113], and that an increase in L leads to a sharp increase in the diffraction losses (see also [243]). We note that the analysis and interpretation of numerous experimental results on the angular divergence of laser emission, for lasers using such an inhomogeneous material as ruby, are frequently quite difficult, since these results depend not only on the concrete form of

the inhomogeneities in the crystals employed, but also on the magnitude (and distribution) of the light scattering in the matter. The role of light scattering in the formation of the angular divergence of laser emission is quite large [52,16], but the influence of light scattering has not yet been investigated theoretically. This influence was studied experimentally in [16] for lasers with $CaF_2:Sm^{2+}$ crystals, which, being macroscopically just as homogeneous as neodymium glass, have appreciable light scattering (0.02—0.04 cm^{-1}). The dependence of the angular divergence α and the generation power P on the resonator length is shown in Fig. 23. We see that α is quite large for small values of L, and varies with the resonator length in proportion to $1/\sqrt{L}$. A decrease in the angular divergence, down to values $\sim 2\alpha_d$, is not accompanied by an appreciable increase in the laser emission power. The relatively large angular divergence of the emission in the presence of light scattering is due apparently to the formation of coupled modes with a large overall angular divergence (see also [52,298]). The coupling between the individual modes of a planar resonator in such a set of modes is effected by the scattered radiation, and is quite weak, in view of the relatively low intensity of this radiation, thus making it possible to reduce the angular divergence without entailing appreciable radiation power losses. Similar concepts can explain qualitatively the $\alpha \sim 1/\sqrt{L}$ dependence, and also the formation of rings around the central spot [16]. The angular radius and the width of such rings correspond to the radius and width of the Fabry-Perot interferometer rings, since the planar resonator acts like such an interferometer for radiation with a frequency equal to the emission frequency in the central spot (see, for example, [16,238,244]). These data, and also the results of [245], show that the formation of rings is a result of interference and amplification of the scattered light, and it is apparently more correct to speak of complex coupled modes whose radiation fills both the central spot and the rings [245,16].

In addition to angular-mode selection by increasing the resonator length, different angular selectors are used to increase the losses for the angular modes. The operation of a selector with a Fabry-Perot interferometer is based on the fact that the transmission of the interferometer depends not only on the wavelengths but also on the direction of the radiation, and therefore the Q of modes with a large directivity pattern turns out to be considerably reduced if a suitably selected and adjusted interferometer is introduced into the resonator. The use of two interferometers, in which selection in two mutually perpendicular directions is effected, has reduced the angular divergence of a ruby laser with a low-grade ruby to 4′ [246]. The operating principle of the selector shown in Fig. 24a is based on the fact that the reflection coefficient of the interface between two media depends strongly on the angle of incidence near the critical total internal reflection angle [247]. To make the dependence of the Q on the angle more acute, it is possible to use multiple reflections (see, for example, [175]). The operating principle of selectors with reflecting spheres (Fig. 24b) [248] and with a diaphragm inside a telescopic system (Fig. 24c) [249] is clear from the figure. These two schemes entail an undesirable increase of the radiation concentration in a small cross section, and therefore offer little promise. It was proposed in [250] to increase the selecting properties of the resonator by depositing the reflecting coatings only on the central part of the mirror. This increases the diffraction losses of all the modes (this is precisely the cause of the selecting action), but the radiation which passes, as a result of diffraction, through the uncoated section is superimposed on the radiation passing through the central semitransparent section, and is therefore part of the useful laser emission. The use of such a selection method in a ruby laser makes it possible to obtain an angle $\alpha \simeq \alpha_d$ at a threshold ratio 2.5, and to increase the axial brightness by a factor of 15 [212]. To obtain generation at a lower angular mode, one frequently uses a spherical resonator of such a configuration, that the transverse cross section of the lowest mode is equal to the cross section of the active rod [299]. We note that in accordance with [279] the angular divergence α in a laser with spherical mirrors is determined by the angular divergence of the mode whose transverse dimension is equal to the rod diameter.

5. Temporal Characteristics of Laser Emission

The most typical of solid-state lasers operating in the pulsed or continuous regime is the "spike" generation regime, in which a time scan of the radiation intensity comprises a set of random oscillations—spikes. It should be noted that such a regime was observed for all active media using solid-state lasers, without exception.* At first, attempts were made to relate the radiation spikes with the transients involved in the establishment of the stationary generation regime. It follows from a solution of the kinetic equations for the single-mode case that there should be observed at the start of the laser operation periodic damped oscillations of radiation intensity, with a period $T_0 \simeq 2\pi\sqrt{\tau t_r/(n-1)}$ (four-level scheme) and an attenuation constant $t_0 \approx 2\tau/n$, where $t_r = 2L\kappa/C(\sigma + \ln 1/R)$ is the lifetime of the photon in the resonator, n is the threshold ratio (see, for example, [18]). Similar expressions for T_0 and t_0 can be obtained also for a three-level medium (see [252]).

*It is assumed in many papers (see, for example, [251]) that $CaF_2:Sm^{2+}$ does not produce spike generation. It has been shown in [52], however, that spikes are produced in this material, too.

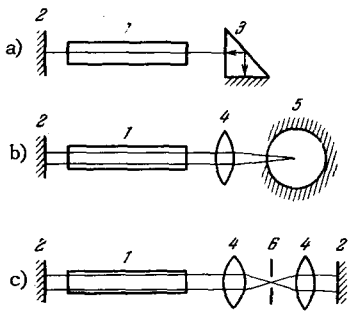

FIG. 24. 1 – Active sample, 2 – mirror, 3 – prism with total internal reflection, 4 – lens, 5 – reflecting sphere, 6 – diaphragm.

The experimentally observed dependence of the average time interval between the random spikes on the generation condition has turned out to be qualitative similar to the corresponding dependence of T_0 (see, for example, [253,254]). However, the irregularity of the spikes and the lack of a tendency for their damping, even in the case of continuous generation, have made it necessary to search for another explanation of the spike regime (see below). Under certain conditions, a spikeless generation regime can be obtained, in which the summary radiation intensity is constant or fluctuates insignificantly about a stationary value. Establishment of this regime is usually accompanied by damped regular pulsations of the radiation, in full agreement with the already indicated single-mode model [93,255-259].

A spikeless generation regime is observed, as a rule, under the following conditions: 1) The resonator is spherical and confocal [260-262], concentric [254,259,263-266], and also in the form of a torus [267]*. 2) The temperature of the active rod is low. A spikeless regime was observed at low temperatures for ruby [254], $CaF_2:Sm^{2+}$ [52], and $CaF_2:Dy^{2+}$ [63]. 3) The resonator length is large [255,254] and the resonator losses small [256,262]. A smooth generation pulse was observed also following axial mode selection [270] and in a unidirectional ring laser [93]. It is shown in [262] that an important parameter determining the generation regime is the ratio t_0/T_0.

When $t_0/T_0 < 10$, damped radiation pulsations, which went over into the spikeless regime, were observed, when t_0/T_0 increased the operation became less regular, and when $t_0/T_0 \gtrsim 50$ the spikes were utterly random. In particular, more regular operation was obtained by an increase in the pump intensity, since it decreased t_0/T_0 (for example, [264,265]). An intermediate position between the operating regimes described above is that of undamped regular pulsations, observed as a rule when the resonator has spherical mirrors* [263,264,268]. It has been established that when the mirrors are gradually moved from the concentric position, the generation regime goes over from the spikeless one to regular pulsations and eventually to random spikes [263,264,266]. We note that in the case of regular pulsations, the generation contains simultaneously a large number of modes distributed in a broader spectral range than in the case of the irregular regime [265,266].

In conclusion, we shall dwell briefly on attempts to interpret the foregoing experimental observation. In a number of theoretical papers, the regime of undamped pulsations was described by taking into account the off diagonal element of the density matrix. In view of the complexity of the initial equations, this method was used to consider, in the main, generation at one [18] or two [8,19] modes, which is insufficient for a quantitative interpretation of the experimental data.

The temporal characteristics of the generation were considered in [5,6] in a multimode approximation of the model of kinetic equations, with account taken of the spatial structure of the emission. Although the numerical calculations presented for different laser parameters led in all cases only to damped oscillations of the radiation, the behavior of such oscillations during the transient time turned out to be similar in many respects to the behavior of the experimentally observed spikes. In particular, their regularity exhibited a similar dependence on t_0/T_0.

To explain the random pulsations, it was proposed in [272] to take into account the fluctuations in the energy delivered to individual modes by the spontaneous emission. Favoring such a notion is, in particular, the absence of coherence between individual emission spikes.

Other attempts were also made to interpret the undamped pulsations of laser emission within the framework of the probability method (see, for example, [272,273]). These attempts were so far not successful, possibly because of the fact that the probability method is not adequate in principle for description of the temporal characteristics of laser emission.

The temporal characteristics of Q-switched lasers, and particularly lasers operating in the monopulse regime, are determined both by the parameters of the shutter, resonator, or active medium, and by the processes of interaction between the excited modes. Insufficient speed of switching can lead to an appearance of several generation pulses (see Sec. III, 4). The duration of the pulse from a monopulse laser is usually 10–50 nsec [27,172,174,180,181]. A number of investigations have established that these pulses have

*Observation of a spikeless regime was also reported for the case of a planar resonator (see, for example, [268,269]). It is possible that in this case the sphericity of the resonator was maintained by inhomogeneities in the crystal or by thermal deformation.

*Undamped pulsations were observed also with the ruby placed in an immersion liquid [271] and when fibers of neodymium-activated glass were used [219].

a temporal fine structure determined by the interaction between the modes [289,290]. A theoretical analysis of the dynamics of pulse formation in a monopulse laser, with allowance for the interaction between the angular modes and for the uneven distribution of the inversion over the cross section of the rod, has shown that the pulse delivered by the entire end surface of the laser is the envelope of pulses emitted by individual sections of the crystal [228]. This circumstance was experimentally confirmed in [291,292]. The interaction of the axial modes in the case of Q-switching of a laser by a passive shutter [293-295] (self-capture of modes) or internal ultrasonic modulation at a frequency which is a multiple of $C/2L$ [296,297], makes it possible to obtain a series of ultrashort pulses (10^{-10} sec), whose duration is shorter than the time of flight of the quantum in the resonator. The self-capture effect is apparently due to modulation of the transmission of the passive shutter, resulting from field-intensity pulsations caused by mixing of the axial-mode frequencies in the nonlinear medium of the shutter. The use of the mode self-capture effect and a scheme for rapidly shutting off the resonator mirror [35] (see Sec. III, 4) resulted in single generation pulses of duration 8×10^{-10} sec [287]. According to an estimate given in in [294], the limiting pulse durations that can be obtained as a result of the mode self-capture effect are $\sim 5 \times 10^{-13}$ sec.

[1] A. L. Shawlow and C. H. Townes, Phys. Rev. **112**, 1940 (1958).

[2] A. G. Fox and T. Li, Bell Syst. Techn. J. **40**, 453 (1961).

[3] G. D. Boyd and J. P. Gordon, Bell Syst. Techn. J. **40**, 489 (1961).

[4] L. A. Vaĭnshtein, Zh. Eksp. Teor. Fiz. **44**, 1050 (1963) and **45**, 684 (1964) [Sov. Phys.-JETP **17**, 709 (1963) and **18**, 471 (1964)].

[5] C. L. Tang, H. Statz, and G. de Mars, J. Appl. Phys. **34**, 2289 (1963).

[6] H. Statz and C. L. Tang, J. Appl. Phys. **35**, 1377 (1964).

[7] Y. H. Pao, JOSA **52**, 871 (1962); Z. Phys. **179**, 393 (1964).

[8] J. A. Fleck and R. E. Kidder, J. Appl. Phys. **35**, 2825 (1964).

[9] T. H. Maiman, Phys. Rev. **123**, 1145 (1961).

[10] A. M. Prokhorov, Radio i élektronika **8**, 1073 (1963).

[11] Yu. A. Anan'ev, V. F. Egorova, A. A. Mak, D. S. Prilezhaev, and B. M. Sedov, Zh. Eksp. Teor. Fiz. **44**, 1884 (1963) [Sov. Phys.-JETP **17**, 1268 (1963)].

[12] B. I. Stepanov and V. P. Gribkovskiĭ, Usp. Fiz. Nauk **82**, 201 (1964) [Sov. Phys.-Usp. **7**, 68 (1964)].

[13] A. L. Mikaelyan, M. L. Ter-Mikaelyan, and Yu. G. Turkov, Radio i élektronika **9**, 1788 (1964).

[14] B. L. Livshitz, S. N. Stolyarov, and V. N. Tsikunov, Dokl. Akad. Nauk SSSR **168**, 72 (1966) [Sov. Phys.-Dokl. **11**, 412 (1966)].

[15] Yu. A. Anan'ev, Zh. Tekh. Fiz. **37**, 139 (1967) [Sov. Phys.-Tech. Phys. **12**, 97 (1967)].

[16] Yu. A. Anan'ev, A. A. Mak, and B. M. Sedov, Zh. Eksp. Teor. Fiz. **52**, 12 (1967) [Sov. Phys.-JETP **25**, 6 (1967)].

[17] H. Haken and H. Sauermann, Z. Phys. **173**, 261 (1963); **176**, 47 (1963).

[18] A. N. Oraevskiĭ and A. V. Uspenskiĭ, Trudy FIAN (Physics Institute, Acad. Sci. SSSR) **31**, 96 (1965).

[19] N. G. Basov, V. N. Morozov, and A. N. Oraevskiĭ, Dokl. Akad. Nauk SSSR **162**, 781 (1965) [Sov. Phys.-Dokl. **10**, 516 (1965)]; Zh. Eksp. Teor. Fiz. **49**, 895 (1965) [Sov. Phys.-JETP **22**, 622 (1966)].

[20] V. S. Mashkevich, Osnovy kinetiki izlucheniya lazerov (Principles of Laser Emission Kinetics) Kiev, Naukova dumka, 1966.

[21] B. I. Stepanov, A. P. Ivanov, B. M. Berkovskiĭ, and I. L. Katsev, Opt. Spektrosk. **12**, 533 (1962).

[22] A. L. Mikaelyan, M. L. Ter-Mikaelyan, and Yu. G. Turkov, Radio i élektronika **9**, 1357 (1964).

[23] Yu. A. Anan'ev, V. P. Gribkovskiĭ, A. A. Mak, and B. I. Stepanov, Dokl. Akad. Nauk SSSR **150**, 507 (1963) [Sov. Phys.-Dokl. **8**, 471 (1963)].

[24] A. Jariv and I. P. Gordon, Proc. IEEE **51**, 4 :9 (1963).

[25] A. Jariv, Proc. IEEE **51**, 1723 (1963).

[26] N. M. Galaktionova, V. F. Egorova, V. S. Zubkova, A. A. Mak, and D. S. Prilezhaev, Dokl. Akad. Nauk SSSR **174**, No. 3 (1967) [sic!].

[27] F. McClung and R. Hellwarth, Proc. IEEE **51**, 46 (1963).

[28] Yu. A. Anan'ev, A. A. Mak, and B. M. Sedov, Zh. Eksp. Teor. Fiz. **48**, 7 (1965) [Sov. Phys.-JETP **21**, 4 (1965)].

[29] B. A. Ermakov, A. V. Lukin, and A. A. Mak, Opt. Spektrosk. **18**, 353 (1965).

[30] T. K. Razumova, ibid. **20**, 360 (1966).

[31] T. T. Waite, J. Appl. Phys. **35**, 1680 (1964).

[32] J. A. Fleck, J. Appl. Phys. **36**, 1301 (1965).

[33] Yu. A. Anan'ev, I. F. Balashov, and A. A. Mak, Dokl. Akad. Nauk SSSR **166**, 825 (1966) [Sov. Phys.-Dokl. **11**, 124 (1966)].

[34] A. J. De Maria, J. Appl. Phys. **34**, 2296 (1963).

[35] A. A. Vuylsteke, J. Appl. Phys. **34**, 1615 (1963).

[36] W. G. Wagher and B. A. Langyel, J. Appl. Phys. **34**, 2040 (1963).

[37] A. L. Mikaelyan and Yu. G. Turkov, Radio i élektronika **9**, 743 (1964).

[38] M. Menat, J. Appl. Phys. **36**, 73 (1965).

[39] R. Kay and G. Waldman, J. Appl. Phys. **36**, 1319 (1965).

[40] T. V. Gveladze, I. K. Krasyuk, P. P. Pashinin, A. V. Prokhindeev, and A. M. Prokhorov, Zh. Eksp. Teor. Fiz. **48**, 106 (1965) [Sov. Phys.-JETP **21**, 72 (1965)].

[41] J. E. Geusic and H. Scovil, Bell Syst. Techn. J. 41, 1371 (1962).
[42] L. Frantz and J. Nodvik, J. Appl. Phys. 34, 2346 (1963).
[43] J. Wittke, J. Appl. Phys. 35, 1668 (1964).
[44] A. E. Siegman, J. Appl. Phys. 35, 460 (1964).
[45] N. G. Basov and V. S. Letokhov, Opt. Spektrosk. 18, 1042 (1965).
[46] N. G. Basov, R. V. Ambartsumyan, V. S. Zuev, P. G. Kryukov, and V. S. Letokhov, Zh. Eksp. Teor. Fiz. 50, 23 (1966) [Sov. Phys.-JETP 23, 16 (1966)].
[47] N. G. Basov, A. Z. Grasyuk, and I. G. Zubarev, Dokl. Akad. Nauk SSSR 157, 1084 (1964) [Sov. Phys.-Dokl. 9, 678 (1965)].
[48] N. V. Karlov and A. M. Prokhorov, Radio i elektronika 11, 267 (1966).
[49] J. Castro, F. A. Brand, C. LoCasio, S. Weitz, and G. Novick, JOSA 56, 149 (1966).
[50] E. I. Antoshina, N. A. Kozlov, A. A. Mak, A. I. Stepanov, and D. S. Prilezhaev, Zh. Prikladnoi spektroskopii (J. of Applied Spectroscopy) 5, 167 (1966).
[51] T. I. Kuznetsova and S. G. Rautian, Fiz. Tverd. Tela 5, 2105 (1963) [Sov. Phys.-Solid State 5, 1535 (1964)].
[52] Yu. A. Anan'ev and B. M. Sedov, Zh. Eksp. Teor. Fiz. 48, 782 (1965) [Sov. Phys.-JETP 21, 517 (1965)].
[53] B. L. Livshitz and V. N. Tsikunov, ibid. 49, 1843 (1965) [22, 1260 (1966)].
[54] B. L. Livshitz and V. N. Tsikunov, Dokl. Akad. Nauk SSSR 162, 314 (1965) and 163, 870 (1965) [Sov. Phys.-Dokl. 10, 446 (1965) and 745 (1966)].
[55] A. A. Kaminski and V. V. Osiko, Neorganicheskie materialy (Inorganic Materials) 1, 2049 (1965).
[56] P. P. Feofilov, Izv. AN SSSR ser. fiz. 26, 435 (1962).
[57] P. P. Feofilov, A. M. Bonch-Bruevich, V. V. Vargin, Ya. A. Imas, G. O. Karapetyan, Ya. E. Kariss, and M. N. Tolstoi, ibid. 27, 466 (1963).
[58] K. Nassau, Proc. Symp. Opt. Masers, N.Y., 1963.
[59] L. F. Johnson and R. A. Thomas, Phys. Rev. 131, 2038 (1963).
[60] J. Geusic, H. Markos, L. Van Uitert, Appl. Phys. Letts 4, 182 (1964).
[61] Z. I. Kiss and R. C. Dunkan, Appl. Phys. Letts 5, 198 (1964).
[62] P. P. Feofilov, V. A. Timofeeva, M. N. Tolstoĭ, and L. M. Belyaev, Opt. Spektrosk. 19, 817 (1965).
[63] Z. I. Kiss and R. C. Dunkan, Proc. IRE 50, 1531 (1962).
[64] Z. I. Kiss, Phys. Rev. 137A, 1749 (1965).
[65] V. K. Konyukhov, V. V. Kostin, L. A. Kulevskiĭ, T. M. Murina, and A. M. Prokhorov, Dokl. Akad. Nauk SSSR 165, 1056 (1965) [Sov. Phys.-Dokl. 10, 1192 (1966)].
[66] N. M. Galaktionova, V. F. Egorova, V. S. Subkova, and A. A. Mak, Opt. Spektrosk. 22, 68 (1967). Paper at Symposium on the Spectroscopy of Crystals Containing Rare-earth and Iron-group Elements, Moscow, 1965.
[67] W. Kaiser, C. Garrett, and D. Wood, Phys. Rev. 123, 766 (1961).
[68] T. H. Maiman, R. H. Hoskins, I. J. D'Haenens, C. K. Asawa, and V. Evtuhov, Phys. Rev. 123, 1151 (1961).
[69] A. L. Schawlow, Advances in Quantum Electronics, N.Y.—London, 50 (1961).
[70] G. O. Karapetyan, Ya. E. Kariss, S. G. Lunter, and P. P. Feofilov, Zh. prikladnoi spektroskopii (J. of Applied Spectroscopy) 1, 1 (1964).
[71] K. Hauptmanowa, J. Pantoflicek, and K. Patek, Phys. Stat. Sol. 9, 525 (1965).
[72] F. Gires and G. Mayer, Proc. 3d Intern. Congr. Quant. Electron, Paris, N. Y., 1964.
[73] M. D. Galanin, V. N. Smorchkov, and Z. A. Chizhikova, Opt. Spektrosk. 19, 296 (1965).
[74] A. M. Bonch-Bruevich, T. K. Razumova, and Ya. A. Imas, ibid. 20, 1040 (1966).
[75] R. C. Vickery, Proc. 3d Intern. Congr. Quant. Electron, Paris, N. Y., 1964.
[76] V. F. Egorova, V. S. Zubkova, G. O. Karapetyan, A. A. Mak, D. S. Prilezhaev, and A. A. Reishakhrit, Opt. Spektrosk. 23 (1967); Paper at XIV Conference on Luminescence, Riga, 1965.
[77] D. W. Harper, Phys. und Chem. Glasses 5, 11 (1964).
[78] T. Kamogawa and H. Kotera, Jap. J. Appl. Phys. 5, 449 (1966).
[79] P. P. Feofilov and A. A. Kaplyanskiĭ, Usp. Fiz. Nauk 76, 201 (1962) [Sov. Phys.-Usp. 5, 79 (1962)].
[80] S. Porto and A. Jariv, Proc. 3d Intern. Congr. Quant. Electron., Paris—N.Y., 1964.
[81] V. F. Egorova, V. S. Zubkova, A. A. Mak, and D. S. Prilezhaev, Opt. Spektrosk. 20, 890 (1966).
[82] Yu. K. Voron'ko, A. A. Kaminskiĭ, and V. V. Osiko, Zh. Eksp. Teor. Fiz. 49, 420 (1965) [Sov. Phys.-JETP 22, 295 (1966)].
[83] Ya. E. Kariss, M. N. Tolstoĭ, and P. P. Feofilov, Opt. Spektrosk. 18, 440 (1965).
[84] E. E. Bukke and Z. L. Morgenshtern, ibid. 14, 687 (1963).
[85] Z. L. Morgenshtern and V. V. Neustruev, ibid. 20, 837 (1966).
[86] L. G. Deshazer and L. F. Komai, JOSA 55, 940 (1965).
[87] L. F. Johnson, Proc. 3d Intern. Congr. Quant. Electron, Paris—N.Y., 1964.
[88] N. M. Galaktionova, V. F. Egorova, V. S. Zubkova, A. A. Mak, and D. S. Prilezhaev, Opt. Spektrosk. 23, (1967).
[89] J. A. Konigstein, and J. E. Geusic, Phys. Rev. 136, 711 (1964).
[90] A. L. Shawlow, Proc. 3d Intern. Congr. Quant. Electron, Paris—N.Y., 1964.
[91] D. E. McCumber and M. D. Sturge, J. Appl. Phys. 34, 1682 (1963).

[92] B. Z. Malkin, Fiz. Tverd. Tela 5, 1062 (1963) [Sov. Phys.-Solid State 5, 773 (1963)].
[93] C. L. Tang, H. Statz, G. A. de Mars, and D. T. Wilson, Phys. Rev. 136A, 1 (1964).
[94] Yu. A. Anan'ev, A. A. Mak, and B. M. Sedov, Zh. prikladnoĭ spektroskopii (J. of Applied Spectroscopy) 1, 169 (1964).
[95] N. M. Galaktionova, V. F. Egorova, and A. A. Mak, Zh. Eksp. Teor. Fiz. 49, 1068 (1965) [Sov. Phys. JETP 22, 743 (1966)].
[96] N. M. Galaktionova, V. F. Egorova, A. A. Mak, and D. S. Prilezhaev, Paper at XIV Conference on Luminescence, Riga, 1965.
[97] J. K. Wright, C. H. H. Catmichael, and B. J. Brown, Phys. Letts 16, 264 (1965).
[98] W. Kecne and J. Weiss, Appl. Opt. 3, 545 (1964).
[99] M. Michon, J. Ernest, R. Dumamchin, J. Hanns, and S. Roynand, Phys. Letts 19, 217 (1965).
[100] L. F. Johnson, J. E. Geusic, and L. G. Van Uitert, Appl. Phys. Letts 7, 127 (1965).
[101] S. Shiohoja and E. Nakazawa, Appl. Phys. Letts 6, 117 (1965).
[102] N. T. Melamed, C. Hirayama, and E. K. Davis, Appl. Phys. Letts 7, 170 (1965).
[103] H. W. Gandy, R. J. Ginther, and J. F. Weller, Phys. Letts 11, 213 (1964).
[104] I. J. D'Haenens and C. R. Giuliano, IEEE J. Quant. Electron 1, 393 (1965).
[105] O. N. Voron'ko, N. A. Kozlov, A. A. Mak, B. G. Malinin, and B. I. Stepanov, Dokl. Akad. Nauk SSSR 173, 542 (1967) [Sov. Phys.-Dokl. 12, in press].
[106] D. G. Grant, Proc. IEEE 51, 604 (1963).
[107] G. D. Boyd, and H. Kogelnik, Bell. Syst. Techn. J. 41, 1347 (1962).
[108] A. M. Leontovich and A. P. Veduta, Zh. Eksp. Teor. Fiz. 46, 71 (1964) [Sov. Phys.-JETP 19, 51 (1964)].
[109] R. V. Pole, JOSA 55, 254 (1965).
[110] A. G. Fox and T. Li, Proc. IEEE 51, 80 (1963).
[111] H. Kogelnik, Bell Syst. Techn. J. 44, 439 (1965).
[112] J. Kotik and M. C. Newstein, J. Appl. Phys. 32, 178 (1961).
[113] V. V. Lyubimov, Opt. Spektrosk. 21, 224 (1966).
[114] C. M. Stickley, Appl. Opt. 3, 967 (1964).
[115] T. I. Kuznetsova, Zh. Tekh. Fiz. 34, 419 (1964) and 36, 58 (1966) [Sov. Phys.-Tech. Phys. 9, 330 (1964) and 11, 40 (1966)].
[116] A. F. Suchkov, Zh. Eksp. Teor. Fiz. 49, 1495 (1965) [Sov. Phys.-JETP 22, 1026 (1966)].
[117] H. Statz and C. L. Tang, J. Appl. Phys. 36, 1816 (1965).
[118] M. P. Vanyukov, V. I. Isaenko, and V. A. Serebryakov, Zh. Eksp. Teor. Fiz. 44, 1493 (1963) and 46, 1182 (1964) [Sov. Phys.-JETP 17, 1004 (1963) and 19, 800 (1964)].
[119] I. Ryosuke and I. Hiroshi, Jap. J. Appl. Phys. 4, 231 (1965).
[120] A. N. Oraevskiĭ and V. A. Shcheglov, Radio i élektronika 10, 1140 (1965).
[121] A. Szabo and F. R. Lipsett, Proc. IRE 50, 1690 (1962).
[122] A. M. Bonch-Bruevich, Ya. A. Imas, and A. P. Sokolov, Zh. prikladnoĭ spektroskopii (J. of Applied Spectroscopy) 1, 80 (1964).
[123] D. Findlay and R. A. Clay, Phys. Letts 20, 277 (1966).
[124] B. I. Stepanov, S. A. Mikhnov, and A. N. Rubinov, Zh. prikladnoĭ spektroskopii (J. Applied Spectroscopy) 4, 122 (1966).
[126] A. P. Veduta, A. M. Leontovich, and V. N. Smorchkov, Zh. Eksp. Teor. Fiz. 48, 87 (1965) [Sov. Phys.-JETP 21, 59 (1965)].
[127] R. Townsend, C. Stickley, and A. Maio, Appl. Phys. Letts 7, 94 (1965).
[128] M. P. Vanyukov, V. I. Isaenko, L. A. Luizova, and O. A. Shorokhov, Zh. prikladnoĭ spektroskopii (J. of Applied Spectroscopy) 2, 295 (1965).
[129] Yu. A. Anan'ev, N. A. Kozlov, A. A. Mak, and A. I. Stepanov, ibid. 5, 51 (1966).
[130] S. D. Sims, A. Stein, C. Roth, Appl. Opt. 5, 621 (1966).
[131] L. J. Aplet, E. B. Lay, and W. R. Sooy, Appl. Phys. Letts 8, 71 (1966).
[132] H. Welling, and C. Bickart, Josa 56, 611 (1966).
[133] M. P. Vanyukov and A. A. Mak, Usp. Fiz. Nauk 66, 301 (1958) [Sov. Phys.-Usp. 1, 137 (1959)].
[134] N. M. Galaktionova and A. A. Mak, Opt. Spektrosk. 16, 153 (1964).
[135] V. K. Kanyukhov, L. A. Kulevskii, and A. M. Prokhorov, Zh. prikladnoĭ spektroskopii (J. of Applied Spectroscopy) 1, 51 (1964).
[136] V. F. Egorova, N. A. Kozlov, A. A. Mak, and S. A. Yakovlev, ibid. 1, 294 (1964).
[137] J. Emmett, A. L. Shawlov, and E. H. Weinberg, J. Appl. Phys. 35, 2601 (1964).
[138] P. V. Avizonis and T. Legato, J. Appl. Phys. 36, 3302 (1965).
[139] J. L. Emmett, and A. L. Shawlow, Appl. Phys. Letts 2, 204 (1963).
[140] R. L. Greene, J. L. Emmett, and A. L. Shawlow, Appl. Opt. 5, 350 (1966).
[141] R. A. Brandewie, J. S. Hitt, and J. M. Feldman, J. Appl. Phys. 34, 3415 (1963).
[142] J. S. Hitt and J. M. Feldman, Proc. IEEE 52, 611 (1964).
[143] K. K. Rebane, in: Spektroskopiya kristallov (Spectroscopy of Crystals) (Materials of Symposium on the Spectroscopy of Crystals Containing Rare-earth and Iron-group Elements, Moscow, 1965), Moscow, Nauka, 1966, p. 21.
[144] J. Geusic, M. Hensel, and R. Smith, Appl. Phys. Letts 6, 175 (1965).
[145] L. P. Shishatskaya, Svetotekhnika (Light Technology) 10, 12 (1965).

[146] A. A. Kaminskiĭ, L. S. Kornienko, and A. M. Prokhorov, Dokl. Akad. Nauk SSSR 161, 1063 (1965) [Sov. Phys.-Dokl. 10, 334 (1965)].
[147] N. A. Kozlov, A. A. Mak, and B. M. Sedov, Opt.-Mekh. Prom. No. 11, 25 (1966) [Sov. J. Opt. Tech].
[148] C. G. Young, Appl. Opt. 5, 993 (1966).
[149] G. R. Simpson, Appl. Opt. 3, 780 (1964).
[150] V. Evtuhov and J. K. Neeland, Appl. Phys. Letts 6, 70 (1965).
[151] D. Roess and G. Zeidler, Appl. Phys. Letts 8, 10 (1966).
[152] R. J. Keyes and T. M. Quist, Appl. Phys. Letts 4, 50 (1964).
[153] R. H. Harada and C. K. Suzuki, Appl. Opt. 4, 225 (1965).
[154] J. Ogland, C. Baugh, and W. H. Horn, Appl. Phys. Letts 4, 133 (1964).
[155] V. L. Levshin, E. Ya. Arapova, A. I. Blazhevich, et al., Trudy FIAN (Physics Institute, Acad. Sci. SSSR) 23, 10 (1963).
[156] V. L. Levshin, Paper at XII Conf. on Luminescence, L'vov, 1964.
[157] M. P. Bedilov, V. M. Likhachev, T. V. Mikhailov, and M. S. Rabinovich, ZhETF Pis. Red. 2, 95 (1965) [JETP Lett. 2, 59 (1965)].
[158] O. Svelto, Appl. Opt. 1, 745 (1962).
[159] Yu. A. Anan'ev, PTÉ No. 2, 135 (1964).
[160] V. N. Tsikunov, Opt. Spektrosk. 16, 684 (1964).
[161] E. Sucov, Appl. Opt. 4, 593 (1965).
[162] P. A. Miles and H. E. Edgerton, J. Appl. Phys. 32, 740 (1961).
[163] A. L. Mikaelyan, V. M. Gardash'yan, N. A. Sakharova, and Yu. G. Turkov, Radio i electronika 9, 1542 (1964).
[164] D. Roess, Appl. Opt. 3, 259 (1964).
[165] G. J. Fan and C. B. Smoyer, Appl. Opt. 3, 1277 (1964).
[166] J. P. Lesnick, and C. H. Church, IEEE J. QE-2, 16 (1966); Electron News 14 No. 529 (1966).
[167] H. W. Mockei and R. J. Collins, Appl. Phys. Letts 7, 270 (1965).
[168] N. F. Borrelli and M. L. Charters, J. Appl. Phys. 36, 2172 (1965).
[169] C. Cooke, J. McKenna, and J. Skinner, Appl. Opt. 3, 957 (1964); 3, 963 (1964).
[170] Yu. A. Anan'ev and E. A. Korolev, Opt. Spektrosk. 16, 702 (1964).
[171] F. K. Rutkovskiĭ and V. P. Gribkovskiĭ, Zh. prikladnoĭ spektroskopii (J. of Applied Spectroscopy) 3, 32 (1965).
[172] F. T. Arecchi, G. Potenza, and A. Sona, Nuovo Cimento 34, 1458 (1964).
[173] I. F. Balashov, B. G. Berezin, B. A. Ermakov, and V. V. Konyshev, Zh. prikladnoĭ spektroskopii (J. of Applied Spectroscopy) 7, No. 3 (1967).
[174] N. G. Basov, V. S. Zuev, and Yu. V. Senatskiĭ, Zh. Eksp. Teor. Fiz. 48, 1554 (1965) [Sov. Phys.-JETP 21, 1041 (1965)]; ZhETF Pis. Red. 2, 57 (1965) [JETP Lett. 2, 35 (1965)].
[175] R. Daly and S. D. Sims, Appl. Opt. 3, 1063 (1964).
[176] I. S. Zheludev, Usp. Fiz. Nauk 88, 253 (1966) [Sov. Phys.-Usp. 9, 97 (1966)].
[177] V. A. Shamburov and O. G. Blokh, Radio i élektonika 9, 505 (1964).
[178] E. R. Peressini, Appl. Phys. Letts 3, 203 (1963).
[179] P. G. Tager, Yacheika Kerra (The Kerr Cell), M., Iskusstvo, 1937.
[180] B. H. Soffer, J. Appl. Phys. 35, 2551 (1964).
[181] A. L. Mikaelyan, V. Ya. Anton'yants, V. A. Dolgikh, and Yu. G. Turkov, Radio i élektronika 10, 1350 (1965).
[182] P. P. Sorokin, J. J. Luzzi, J. R. Lankard, and G. D. Pettit, IBM J. Res. Develop. 8, 182 (1964).
[183] J. A. Armstrong, J. Appl. Phys. 36, 471 (1965).
[184] G. Bret and F. Gires, Appl. Phys. Letts 4, 175 (1964).
[185] M. P. Lisitsa, N. R. Kulish, V. I. Geets, and P. N. Koval', Opt. Spektrosk. 20, 508 (1966).
[186] B. H. Soffer and R. Hoskins, Nature 204, 4955 (1964).
[187] V. I. Malyshev, A. S. Markin, and V. S. Petrov, ZhETF Pis. Red. 1, No. 3, 49 (1965) [JETP Lett. 1, 99 (1965)].
[188] M. P. Vanyukov, O. D. Dmitrievskiĭ, V. I. Isaenko, and V. A. Serebryakov, Dokl. Akad. Nauk SSSR 167, 547 (1966) [Sov. Phys.-Dokl. 11, 233 (1966).
[189] B. L. Borovich, V. S. Zuev, and V. A. Shcheglov, Zh. Eksp. Teor. Fiz. 49, 1031 (1965) [Sov. Phys.-JETP 22, 717 (1966)].
[190] A. Szabo and R. A. Stein, J. Appl. Phys. 36, 1562 (1965).
[191] M. Michon, J. Ernest, J. Hanus, and R. Auffret, Phys. Letts 19, 219 (1965).
[192] B. A. Ermakov and A. V. Lukin, Zh. prikladnoĭ spektroskopii (J. of Applied Spectroscopy) 4, 410 (1966).
[193] M. L. Spacht and W. R. Sooy, IEEE J. QE-2, N 4 (1966).
[194] I. A. Adrianova, Yu. V. Popov, and V. E. Terent'ev, Opt. Spektrosk. 19, 307 (1965).
[195] N. C. Nedderman, Proc. IRE 50, 1687 (1962).
[196] R. V. Ambartsumyan, N. G. Basov, V. S. Zuev, P. G. Kryukov, and V. S. Letokhov, ZhETF Pis. Red. 4, 19 (1966) [JETP Lett. 4, 12 (1966)].
[197] Electronics N 20, 46 (1965).
[198] D. N. Bylegzhanin and M. Kh. Zelikman, Radio i élektronika 10, 1147 (1965).
[199] C. R. Guiliano, Appl. Phys. Letts. 5, 137 (1964).
[200] P. V. Avizonis and T. Farrington, Appl. Phys. Letts 7, 205 (1965).
[201] J. Davit and M. Soulie, Compt. Rend. 261, 3567 (1965).
[202] F. M. Bunkin and A. M. Prokhorov, Zh. Eksp. Teor. Fiz. 48, 1084 (1965) [Sov. Phys.-JETP 21, 725 (1965)].
[203] L. F. Johnson and R. A. Thomas, Phys. Rev. 131, 2038 (1963).
[204] A. A. Kaminskiĭ, L. S. Kornienko, and A. M.

Prokhorov, Zh. Eksp. Teor. Fiz. 48, 476 (1965) [Sov. Phys.-JETP 21, 318 (1965)].
[205] V. K. Konyukhov, L. A. Kulevskii, and A. M. Prokhorov, Dokl. Akad. Nauk SSSR 149, 571 (1963) [Sov. Phys.-Dokl. 8, 298 (1963)]; Zh. Eksp. Teor. Fiz. 45, 857 (1963) [Sov. Phys.-JETP 18, 588 (1964)].
[206] T. P. Hughes, Nature 195, 325 (1962); T. P. Hughes, K. M. Joung, Nature 196, 332 (1962).
[207] G. R. Hanes and B. P. Stoichett, Nature 195, 587 (1962).
[208] M. P. Vanyukov, V. I. Isaenko, and V. V. Lyubimov, Opt. Spektrosk. 14, 734 (1963); Zh. Eksp. Teor. Fiz. 44, 1151 (1963) [Sov. Phys.-JETP 17, 778 (1963)].
[209] Yu. A. Anan'ev, N. M. Galaktionova, A. A. Mak, and B. M. Sedov, Opt. Spektrosk. 16, 911 (1964).
[210] B. I. McMurtry, Appl. Opt. 2, 767 (1963).
[211] V. V. Korobkin and A. M. Leontovich, Zh. Eksp. Teor. Fiz. 49, 10 (1965) [Sov. Phys.-JETP 22, 6 (1966)].
[212] V. Evtuhov and J. K. Neeland, IEEE J. QE-1, 7 (1965).
[213] V. V. Korobkin and A. M. Leontovich, Zh. Eksp. Teor. Fiz. 44, 1847 (1963) [Sov. Phys.-JETP 17, 1242 (1963)].
[214] M. S. Lipsett and M. P. W. Strandberg, Appl. Opt. 1, 343 (1962).
[215] V. Evtuhov and J. K. Neeland, Appl. Opt. 1, 517 (1962).
[216] A. A. Kaminskiĭ, L. S. Kornienko, and A. M. Prokhorov, Zh. Eksp. Teor. Fiz. 48, 476 (1965) [Sov. Phys.-JETP 21, 318 (1965)].
[217] B. L. Livshitz, V. P. Nazarov, L. K. Sidorenko, and V. N. Tsikunov, ZhETF Pis. Red. 1, No. 5, 23 (1965) [JETP Lett. 1, 136 (1965)].
[218] V. Evtuhov, and A. E. Siegman, Appl. Opt. 4, 142 (1965).
[219] E. Snitzer, Quant. Electron, Proc. 3d Intern. Congr., N. Y., Columbia Univ. Press, 1964, p. 999.
[220] H. Manger, Appl. Opt. 3, 541 (1964).
[221] H. Heinlein and D. Roess, Proc. IEEE 51, 1667 (1963).
[222] A. M. Kubarev, and V. I. Piskarev, Zh. Eksp. Teor. Fiz. 48, 1233 (1965) [Sov. Phys.-JETP 21, 823 (1965)].
[223] V. K. Konyukhov, L. A. Kulevskiĭ, A. M. Prokhorov, and A. K. Sokolov, Dokl. Akad. Nauk SSSR 158, 824 (1964) [Sov. Phys.-Dokl. 9, 875 (1965)].
[224] J. A. Fleck, J. Appl. Phys. 34, 2297 (1963).
[225] M. Birnbaum, and T. L. Stocker, J. Appl. Phys. 34, 3414 (1963).
[226] I. M. Burch, Proc. 3d Intern. Congr. Quant. Electron, Paris—N. Y., 1964.
[227] H. Manger, H. Rothe, Phys. Letts 12, 182 (1964).
[228] V. S. Letokhov and A. F. Suchkov, Zh. Eksp. Teor. Fiz. 50, 1148 (1966) [Sov. Phys.-JETP 23, 763 (1966)].
[229] V. L. Broude, O. N. Pogorelyĭ, and M. S. Soskin, Dokl. Akad. Nauk SSSR 163, 1342 (1965) [Sov. Phys.-Dokl. 10, 756 (1966)].
[230] F. McClung, S. Schwarz, and F. Meiers, J. Appl. Phys. 33, 3139 (1962).
[231] C. J. Hubbard and E. W. Fisher, Appl. Opt. 3, 1499 (1964).
[232] V. L. Broude, V. I. Kravchenko, N. F. Prokopyuk, and M. S. Soskin, ZhETF Pis. Red. 2, 519 (1965) [JETP Lett. 2, 324 (1965)].
[233] M. P. Vanyukov, V. I. Isaenko, L. A. Luizova, and O. A. Shorokhov, Opt. Spektrosk. 20, 963 (1966).
[234] M. Hercher, Appl. Phys. Letts 7, 39 (1965).
[235] B. B. McFarland, R. H. Hoskins and B. H. Soffer, Nature 207, 1180 (1965).
[236] W. R. Sooy, Appl. Phys. Letts 7, 36 (1965).
[237] B. I. Stepanov, Dokl. Akad. Nauk SSSR 148, 74 (1963) [Sov. Phys.-Dokl. 8, 37 (1963)].
[238] C. M. Stickley, Appl. Opt. 2, 855 (1963).
[239] M. P. Vanyukov, V. I. Isaenko, L. A. Luizova, and O. A. Shorokhov, Zh. prikladnoĭ spektroskopii (J. of Applied Spectroscopy) 2, 415 (1965).
[240] V. Evtuhov and J. K. Neeland, Appl. Opt. 2, 319 (1963).
[241] T. S. Jaseja, M. K. Dheer, and D. Madhavan, Appl. Opt. 4, 1643 (1965).
[242] N. A. Sventsitskaya and L. D. Khazov, Zh. prikladnoĭ spektroskopii (J. of Applied Spectroscopy) 3, 230 (1965).
[243] D. P. Bortfeld, R. S. Congleton, M. Geller, R. C. McComas, L. D. Riley, W. R. Sooy, and M. L. Stitch, J. Appl. Phys. 35, 2267 (1964).
[244] B. P. Stoicheff and A. Szabo, Appl. Opt. 2, 811 (1963).
[245] M. P. Vanyukov, V. I. Isaenko, L. A. Luizova, and O. A. Shorokhov, Zh. Eksp. Teor. Fiz. 48, 3 (1965) [Sov. Phys.-JETP 21, 1 (1965)].
[246] S. A. Collins and G. R. White, Appl. Opt. 2, 448 (1963).
[247] J. A. Giordmaine, W. Kaiser, J. Appl. Phys. 35, 3446 (1964).
[248] A. Ikava, Proc. IEEE 51, 1033 (1963).
[249] I. A. Baker and C. W. Peters, Appl. Opt. 1, 674 (1962).
[250] I. T. LaTourette, S. F. Jacobs, and P. Rabinowitz, Appl. Opt. 3, 981 (1964).
[251] V. M. Faĭn and Ya. I. Khanin, Kvantovaya radiofizika (Quantum Radiophysics), M. Soviet Radio Press, 1965.
[252] M. B. Birnbaum, T. Stocker, and S. L. Welles, Proc. IEEE 51, 854 (1963).
[253] M. D. Galanin, A. M. Leontovich, Z. A. Sviridenkov, V. N. Smorchkov, and Z. A. Chizhikova, Opt. Spektrosk. 14, 165 (1963) [Opt. Spectrosc. 14, 86 (1963)
[254] K. Gürs, Z. Naturforsh. 18a, 510 (1963).
[255] K. Gürs, Z. Naturforsh. 17a, 990 (1962).
[256] K. Gürs, Z. Naturforsh. 18a, 1363 (1963).
[257] M. Katzman and J. W. Strozyk, Proc. IEEE 52,

433 (1964); J. Appl. Phys. 35, 725 (1964).
[258] H. Weber, Phys. Letts 11, 288 (1964).
[259] A. K. Sokolov and T. N. Zubarev, Fiz. Tverd. Tela 6, 2590 (1964) [Sov. Phys.-Solid State 6, 2065 (1965)].
[260] L. F. Johnson, G. D. Boyd, K. Nassau, and R. R. Soden, Proc. IRE 50, 213 (1962); Phys. Rev. 126, 1406 (1962).
[261] M. S. Lipsett and L. Mandel, Nature 197, 547 (1963).
[262] K. Gürs, Phys. Letts 16, 125 (1965); Z. Naturforsh. 20[a], 740 (1965).
[263] R. Pole and H. Wieder, Appl. Opt. 3, 1086 (1964).
[264] A. K. Sokolov and T. N. Zubarev, Dokl. Akad. Nauk SSSR 159, 539 (1964) [Sov. Phys.-Dokl. 9, 1006 (1964)].
[265] V. V. Korobkin, A. M. Leontovich, and M. M. Smirnova, Zh. Eksp. Teor. Fiz. 48, 78 (1965) [Sov. Phys.-JETP 21, 53 (1965)].
[266] H. Wieder, J. Appl. Phys. 37, 615 (1966).
[267] D. Roess, Proc. IEEE 51, 468 (1963).
[268] H. Takuma, Jap. J. Appl. Phys. 2, 197 (1963).
[269] A. Jariv, Proc. IRE 50, 1699 (1962).
[270] D. Roess, Proc. IEEE 52, 196 (1964).
[271] B. I. Davis and D. V. Keller, Appl. Phys. Letts 5, 80 (1964).
[272] A. V. Gaponov and V. I. Bezpalov, Izv. Vuzov, Radiofizika 8, 70 (1965).
[273] R. C. Benson and M. R. Mirarchi, IEEE Trans. Militat. Electron. 8, 13 (1964).
[274] R. J. Driav, E. Garmire, and C. H. Townes, Phys. Rev. Letts 13, 479 (1964).
[275] N. G. Basov and V. S. Letokhov, Dokl. Akad. Nauk SSSR 167, 73 (1966) [Sov. Phys.-Dokl. 11, 222 (1966)].
[276] A. X. Cabezes and P. P. Treat, Appl. Opt. 37, 3556 (1966).
[277] M. I. Dzhibladze, G. A. Zvereva, V. V. Kostin, T. M. Murina, and A. M. Prokhorov, Zh. Eksp. Teor. Fiz. 51, 773 (1966) [Sov. Phys.-JETP 24, 513 (1967)].
[278] A. M. Bonch-Bruevich, V. Yu. Petrun'kin, V. N. Arzumanov, N. A. Esepkina, Ya. A. Imas, S. V. Krushilov, L. N. Pakhomov, and V. A. Chernov, Zh. Tekh. Fiz. 36, 2171 (1966) [Sov. Phys.-Tech. Phys. 11, 1621 (1967)].
[279] A. M. Bonch-Bruevich, N. A. Esepkina, Ya. A. Imas, N. A. Pavlenko, L. N. Pakhomov, V. Yu. Petrun'kin, and S. E. Potapov, ibid. 36, 2175 (1966).
[280] D. Roess and G. Zeidler, Electronics 39, 115 (1966).
[281] J. Ernest, M. Michon, and J. Debrie, Phys. Letts 22, 147 (1966).
[282] W. R. Hood, R. H. Dishington and R. P. Hilberg, Appl. Phys. Letts 9, 125 (1966).
[283] R. C. Eckardt, N. J. Bradford, J. W. Tucker, Appl. Phys. Letts 9, 285 (1966).
[284] N. D. Voropaev and A. N. Oraevskiĭ, Izv. Vuzov, Radiofizika 8, 409 (1965).
[285] S. E. Keats, Laser Focus. 2, 33 (1966).
[286] M. P. Vanyukov, V. A. Venchikov, V. I. Isaenko, and V. A. Serebryakov, Opt.-Mekh. Prom. No. 12, 65 (1966) [Sov. J. Opt. Tech.]
[287] A. W. Penney and H. A. Heynay, Appl. Phys. Letts 9, 257 (1966).
[288] L. D. Khazov and A. N. Shestov, Opt. Spektrosk. 23, (1967) [Opt. Spectrosc. 23, in press].
[289] L. Waszak, Proc. IEEE 52, 428 (1964).
[290] M. Hercher, Appl. Phys. Letts 7, 39 (1965).
[291] R. V. Ambartsumyan, N. G. Basov, V. S. Zuev, P. G. Kryukov, V. S. Letokhov, and O. B. Shatberashvili, Zh. Eksp. Teor. Fiz. 51, 406 (1966) [Sov. Phys.-JETP 24, 272 (1967)].
[292] V. V. Korobkin, A. M. Leontovich, M. N. Popova, and M. Ya. Shcheglov, ZhETF Pis. Red. 3, 301 (1966) [JETP Lett. 3, 194 (1966)].
[293] H. W. Mocker and R. J. Collins, Appl. Phys. Letts 7, 270 (1965).
[294] A. J. De Maria, D. A. Stetser, and H. A. Heynay, Appl. Phys. Letts 8, 174 (1966).
[295] B. H. Soffer and B. B. McFarland, Appl. Phys. Letts 8, 166 (1966).
[296] A. J. DeMaria, C. M. Fernar, G. E. Danielson, Appl. Phys. Letts 8, 22 (1966).
[297] M. DiDomenico, J. E. Geusic, H. M. Marcos, R. G. Smith, Appl. Phys. Letts 8, 180 (1966).
[298] R. V. Ambartsumyan, N. G. Basov, N. G. Kryukov, and V. S. Letokhov, ZhETF Pis. Red. 3, 261 (1966) [JETP Lett. 3, 167 (1966)]; Zh. Eksp. Teor. Fiz. 51, 724 (1966) [Sov. Phys.-JETP 24, 481 (1967)].
[299] D. Roess, Appl. Phys. Letts 8, 109 (1966).
[300] L. A. Vaĭnshteĭn, Otkrytye resonatory i otkrytye volnovody (Open Resonators and Open Waveguides) M., Soviet Radio Press, 1966.

Translated by J. G. Adashko